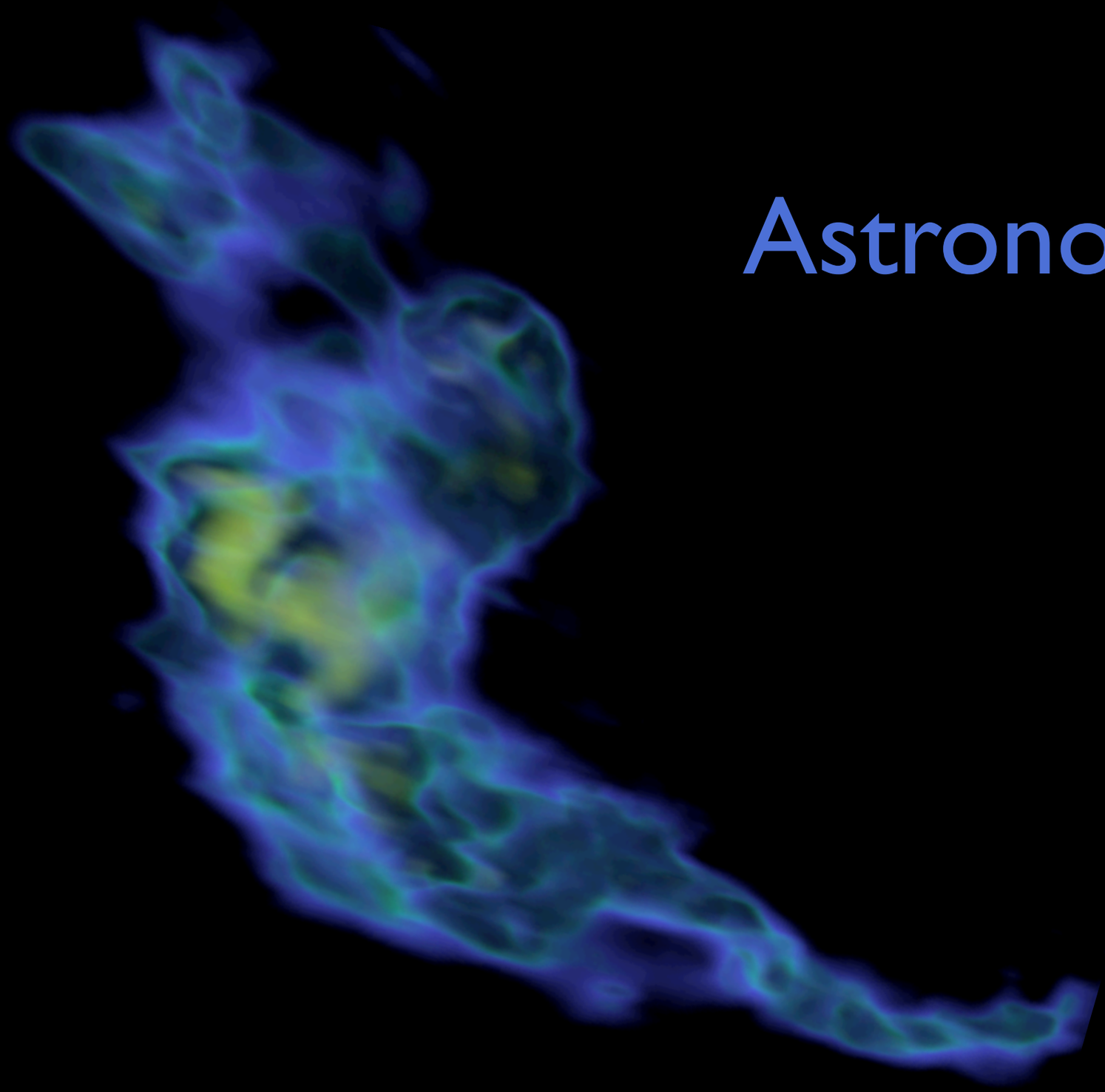

Astronomical Medicine and Beyond

Alyssa A. Goodman

Professor of Astronomy
& Founding Director of the
Initiative in Innovative Computing,
Harvard University

Scholar-in-Residence,
WGBH Boston

Monday, November 16, 2009

Abstract

I will consider the similarities between the imaging modalities and data visualization techniques used in Astronomy and in Medicine. Both fields inherently produce "cubes" or "hyper-cubes" of data where some dimensions are spatial. And, in both fields, tremendous extra value can be derived from visualizing "all" of the data represented in its natural number of dimensions. I will focus on the specific case study where we have used medical imaging software (e.g. 3D Slicer, Osirix) on astronomical observations of star-forming regions to look for the "tumors" (called "dense cores") destined to form new stars like our Sun, and then published our results in *Nature* as that journal's first interactive "3D PDF" interactive paper. I will conclude with a demonstration of the "WorldWide Telescope" program and explain how the natural, "seamless," model of data-literature connections it offers can be extended to other fields.

Science + Technology

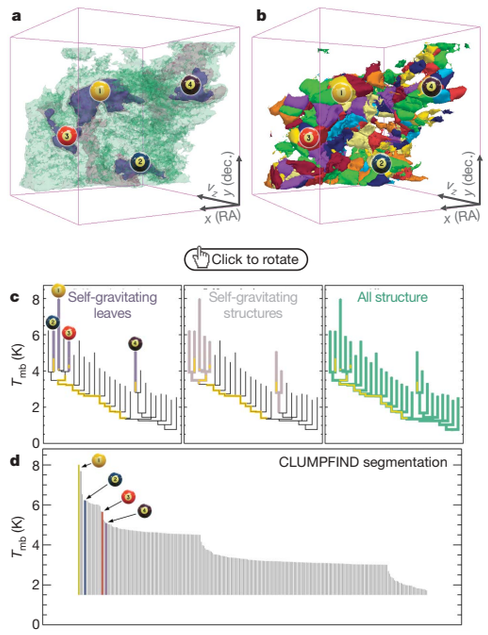

Figure 2 | Comparison of the 'dendrogram' and 'CLUMPFIND' feature-identification algorithms as applied to ^{13}CO emission from the L1448 region of Perseus. a, 3D visualization of the surfaces indicated by colours in the dendrogram shown in **c**. Purple illustrates the smallest scale self-gravitating structures in the region corresponding to the leaves of the dendrogram; pink shows the smallest surfaces that contain distinct self-gravitating leaves within them; and green corresponds to the surface in the data cube containing all the significant emission. Dendrogram branches corresponding to self-gravitating objects have been highlighted in yellow over the range of T_{mb} (main-beam temperature) test-level values for which the virial parameter is less than 2. The *x*–*y* locations of the four 'self-gravitating' leaves labelled with billiard balls are the same as those shown in Fig. 1. The 3D visualizations show position–position–velocity (*p*–*p*–*v*) space. RA, right ascension; dec., declination. For comparison with the ability of dendrograms (**c**) to track hierarchical structure, **d** shows a pseudo-dendrogram of the CLUMPFIND segmentation (**b**), with the same four labels used in Fig. 1 and in **a**. As 'clumps' are not allowed to belong to larger structures, each pseudo-branch in **d** is simply a series of lines connecting the maximum emission value in each clump to the threshold value. A very large number of clumps appears in **b** because of the sensitivity of CLUMPFIND to noise and small-scale structure in the data. In the online PDF version, the 3D cubes (**a** and **b**) can be rotated to any orientation, and surfaces can be turned on and off (interaction requires Adobe Acrobat version 7.0.8 or higher). In the printed version, the front face of each 3D cube (the 'home' view in the interactive online version) corresponds exactly to the patch of sky shown in Fig. 1, and velocity with respect to the Local Standard of Rest increases from front (-0.5 km s^{-1}) to back (8 km s^{-1}).

data, CLUMPFIND typically finds features on a limited range of scales, above but close to the physical resolution of the data, and its results can be overly dependent on input parameters. By tuning CLUMPFIND's two free parameters, the same molecular-line data set[8] can be used to show either that the frequency distribution of clump mass is the same as the initial mass function of stars or that it follows the much shallower mass function associated with large-scale molecular clouds (Supplementary Fig. 1).

Four years before the advent of CLUMPFIND, 'structure trees'[9] were proposed as a way to characterize clouds' hierarchical structure using 2D maps of column density. With this early 2D work as inspiration, we have developed a structure-identification algorithm that abstracts the hierarchical structure of a 3D (*p*–*p*–*v*) data cube into an easily visualized representation called a 'dendrogram'[10]. Although well developed in other data-intensive fields[11,12], it is curious that the application of tree methodologies so far in astrophysics has been rare, and almost exclusively within the area of galaxy evolution, where 'merger trees' are being used with increasing frequency[13].

Figure 3 and its legend explain the construction of dendrograms schematically. The dendrogram quantifies how and where local maxima of emission merge with each other, and its implementation is explained in Supplementary Methods. Critically, the dendrogram is determined almost entirely by the data itself, and it has negligible sensitivity to algorithm parameters. To make graphical presentation possible on paper and 2D screens, we 'flatten' the dendrograms of 3D data (see Fig. 3 and its legend), by sorting their 'branches' to not cross, which eliminates dimensional information on the *x* axis while preserving all information about connectivity and hierarchy. Numbered 'billiard ball' labels in the figures let the reader match features between a 2D map (Fig. 1), an interactive 3D map (Fig. 2a online) and a sorted dendrogram (Fig. 2c).

A dendrogram of a spectral-line data cube allows for the estimation of key physical properties associated with volumes bounded by isosurfaces, such as radius (R), velocity dispersion (σ_v) and luminosity (L). The volumes can have any shape, and in other work[14] we focus on the significance of the especially elongated features seen in L1448 (Fig. 2a). The luminosity is an approximate proxy for mass, such that $M_{lum} = X_{13CO}L_{13CO}$, where $X_{13CO} = 8.0 \times 10^{20}$ cm^2 K^{-1} km^{-1} s (ref. 15; see Supplementary Methods and Supplementary Fig. 2). The derived values for size, mass and velocity dispersion can then be used to estimate the role of self-gravity at each point in the hierarchy, via calculation of an 'observed' virial parameter, $\alpha_{obs} = 5\sigma_v^2 R/GM_{lum}$. In principle, extended portions of the tree (Fig. 2, yellow highlighting) where $\alpha_{obs} < 2$ (where gravitational energy is comparable to or larger than kinetic energy) correspond to regions of *p*–*p*–*v* space where self-gravity is significant. As α_{obs} only represents the ratio of kinetic energy to gravitational energy at one point in time, and does not explicitly capture external over-pressure and/or magnetic fields[16], its measured value should only be used as a guide to the longevity (boundedness) of any particular feature.

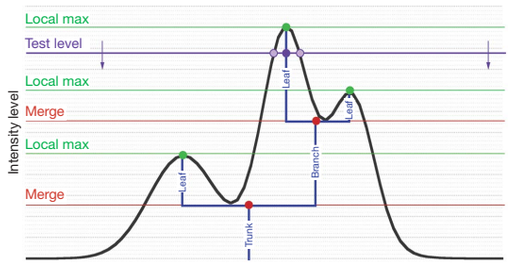

Figure 3 | Schematic illustration of the dendrogram process. Shown is the construction of a dendrogram from a hypothetical one-dimensional emission profile (black). The dendrogram (blue) can be constructed by 'dropping' a test constant emission level (purple) from above in tiny steps (exaggerated in size here, light lines) until all the local maxima and mergers are found, and connected as shown. The intersection of a test level with the emission is a set of points (for example the light purple dots) in one dimension, a planar curve in two dimensions, and an isosurface in three dimensions. The dendrogram of 3D data shown in Fig. 2c is the direct analogue of the tree shown here, only constructed from 'isosurface' rather than 'point' intersections. It has been sorted and flattened for representation on a flat page, as fully representing dendrograms for 3D data cubes would require four dimensions.

©2009 Macmillan Publishers Limited. All rights reserved

Relative Strengths

Pattern Recognition
Creativity

Calculations

“Interocularity”
(see work of John Tukey)
“Image and Meaning”
(see work of Felice Frankel,
and imageandmeaning.org)

What about data visualization...

...is easier now than before?

fast computation, animation, 3D

...was easier before than now?

craftsmanship

...should be easier in the future?

modular craftsmanship

Are we held back by confining tecnological tools?

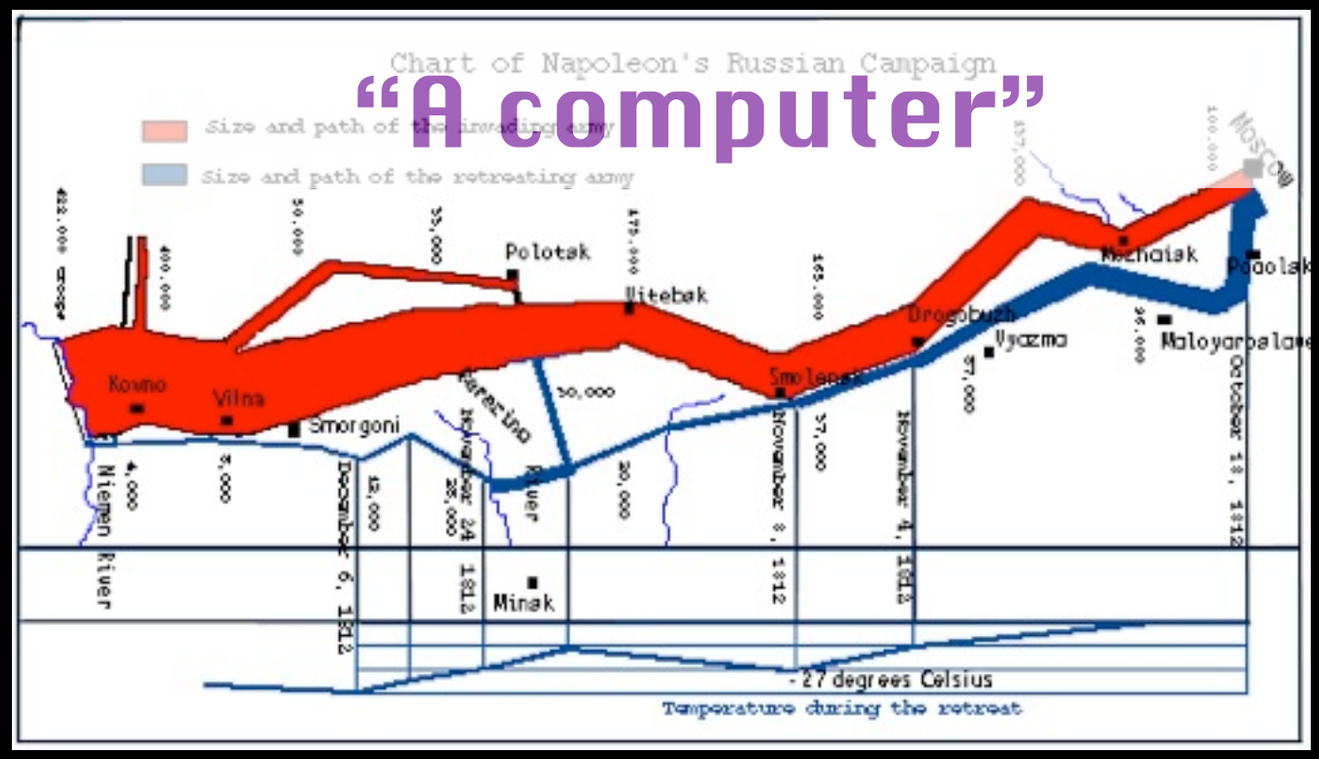

"A computer"

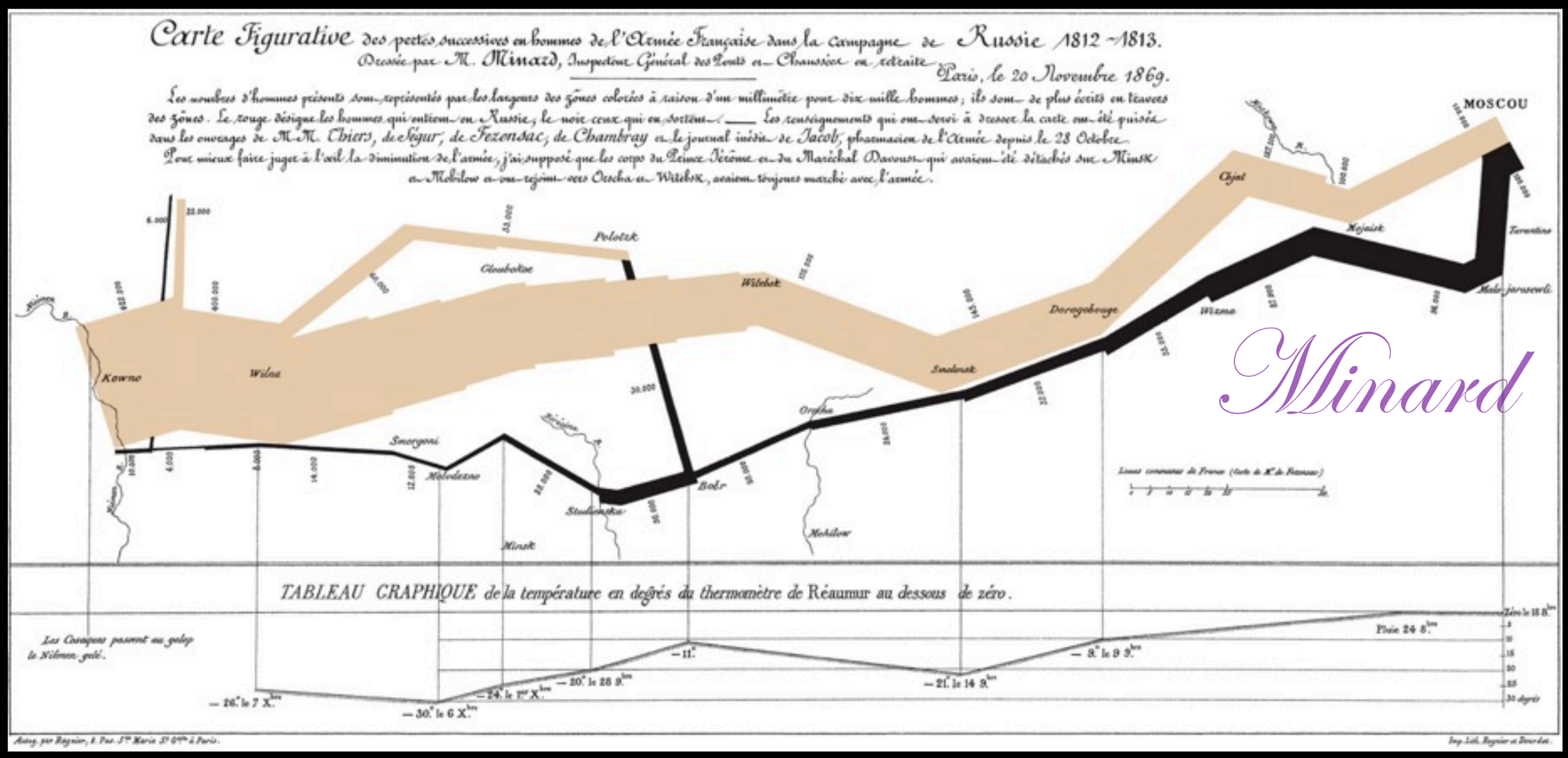

Monday, November 16, 2009

scotch tape story... what about professionals? Minard: 1869; Contest: 1999

Galileo, Science & Technology

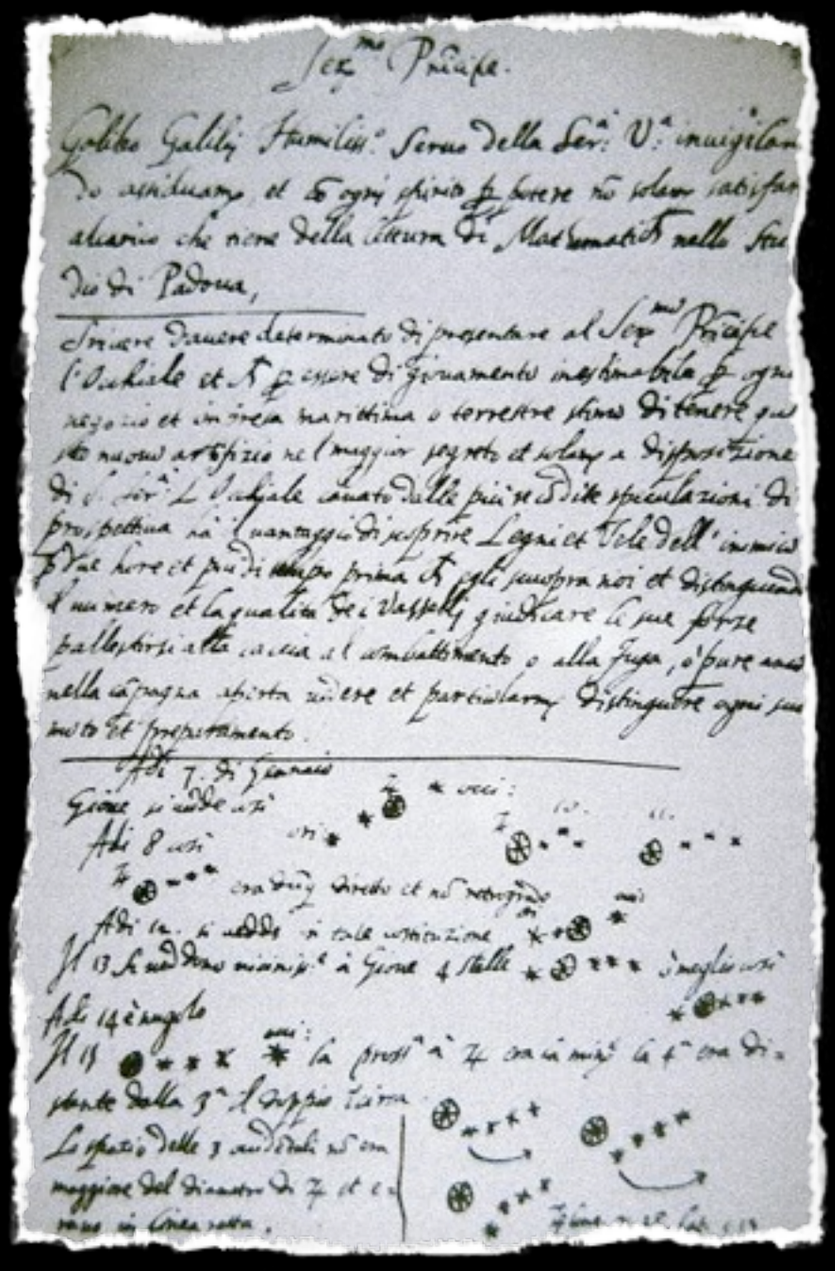
Sec.mo Prencipe.

Galileo Galilej Humilis.mo Servo della Ser.a V.a inuigilan
do assiduamente, et da ogni spirito di buono no solam.te sodisfar
alcuno che nome della Catedra di Mathematich nello Stu
dio di Padoua,

Stimare douere determinato di presentare al Sep.mo Prencipe
l'Vnichiale et N.o essere di giouamento inestimabile di ogni
negotio et in specie marittima o terrestre stimo di tenere que
sto nuouo artefizio nel maggior pregio et stimo a dispositione
di V. Alt.a L'Vnichiale causato dalle prime delle speculazioni di
prospettiua nè i vantaggi di descriue Regni et Prouincie dell'emisfe
ro che vede et più di quello prima di egli scuopra noi et distinguendo
il numero et la qualità de i Vascelli, giudicare le sue forze
ballo per la caccia del combattimento o alla fuga, o pure nella
stessa spiaggia riuolte et particolarm.te distinguere ogni suo
moto et preparamento.

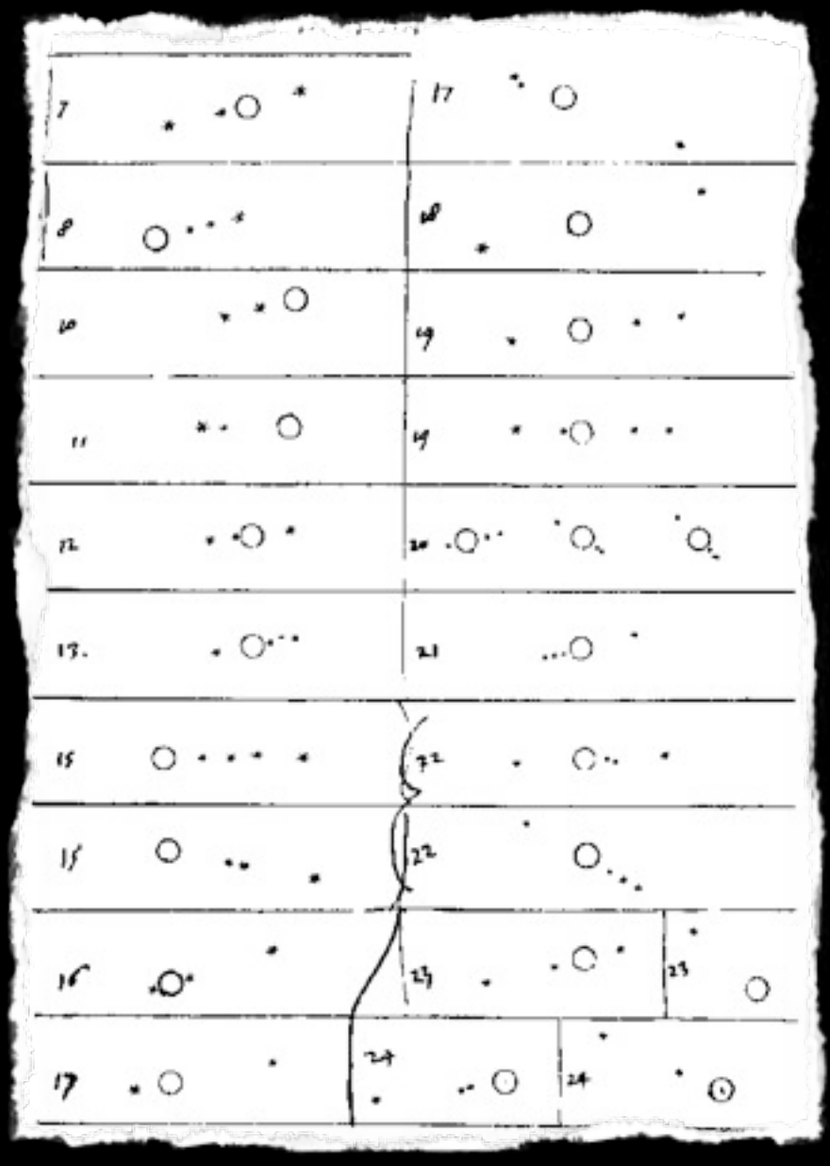

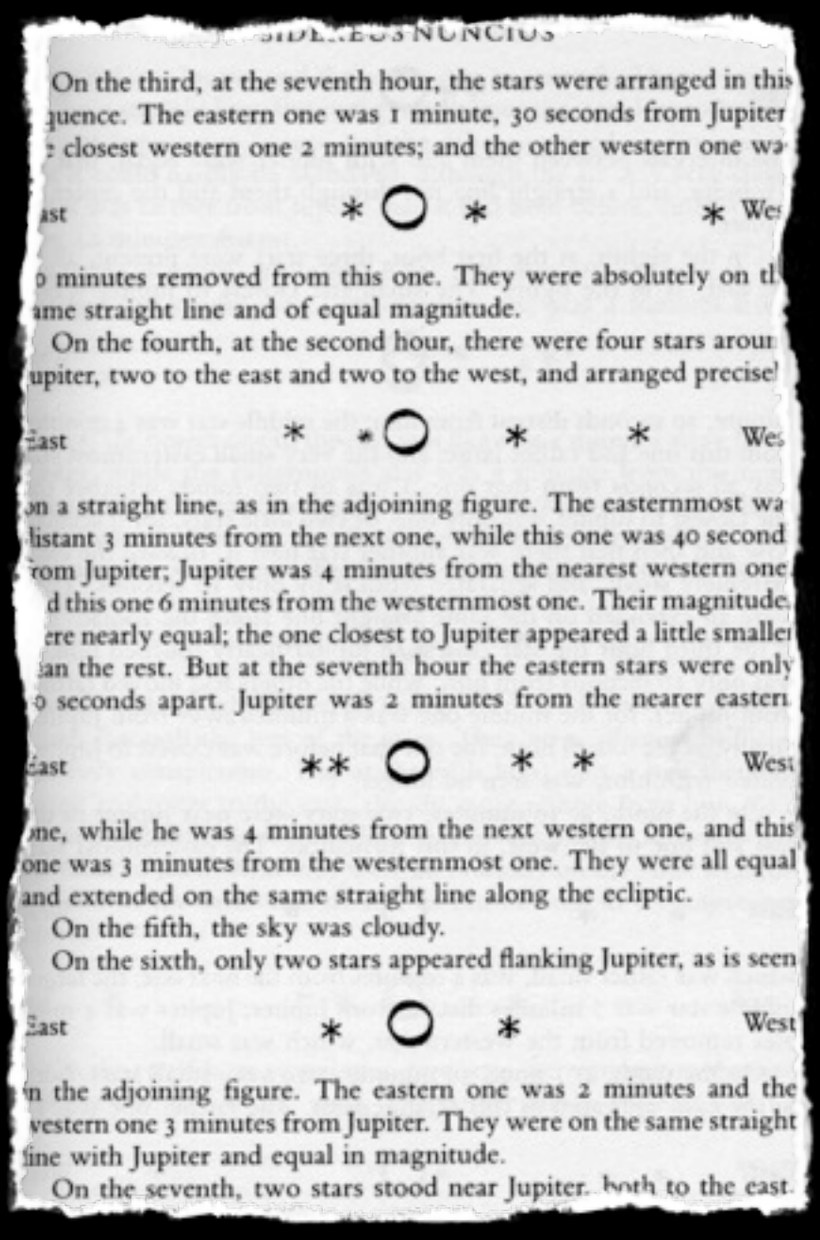
SIDEREUS NUNCIUS

On the third, at the seventh hour, the stars were arranged in this
quence. The eastern one was 1 minute, 30 seconds from Jupiter
closest western one 2 minutes; and the other western one wa

East * ○ * * West

minutes removed from this one. They were absolutely on th
ame straight line and of equal magnitude.

On the fourth, at the second hour, there were four stars aroun
upiter, two to the east and two to the west, and arranged precisel

East * * ○ * * West

on a straight line, as in the adjoining figure. The easternmost wa
listant 3 minutes from the next one, while this one was 40 second
rom Jupiter; Jupiter was 4 minutes from the nearest western one
d this one 6 minutes from the westernmost one. Their magnitude
ere nearly equal; the one closest to Jupiter appeared a little smaller
an the rest. But at the seventh hour the eastern stars were only
o seconds apart. Jupiter was 2 minutes from the nearer eastern

East ** ○ * * West

ne, while he was 4 minutes from the next western one, and this
one was 3 minutes from the westernmost one. They were all equal
and extended on the same straight line along the ecliptic.

On the fifth, the sky was cloudy.

On the sixth, only two stars appeared flanking Jupiter, as is seen

East * ○ * West

n the adjoining figure. The eastern one was 2 minutes and the
western one 3 minutes from Jupiter. They were on the same straight
line with Jupiter and equal in magnitude.

On the seventh, two stars stood near Jupiter, both to the east

Notes for & re-productions of Siderius Nuncius (1610)

Star (and Planet, and Moon) Formation 101

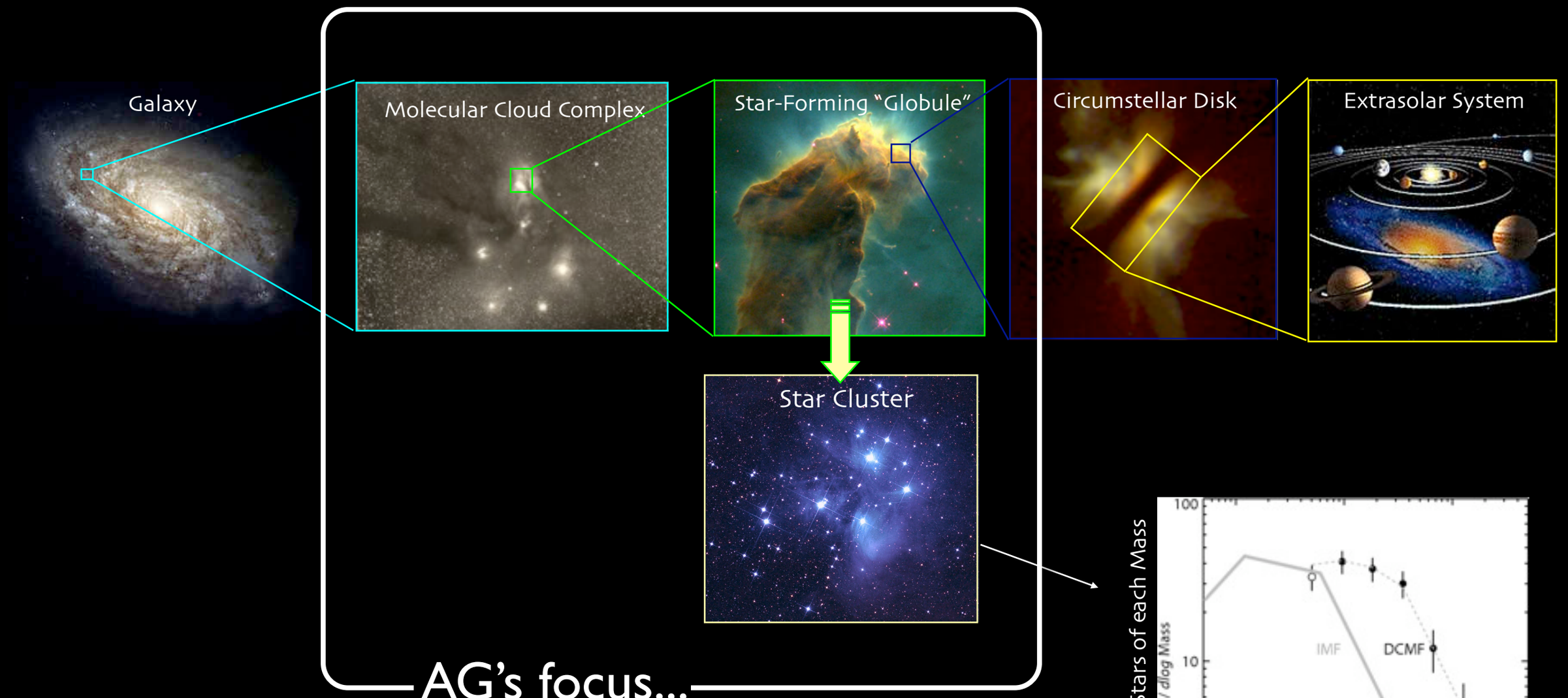

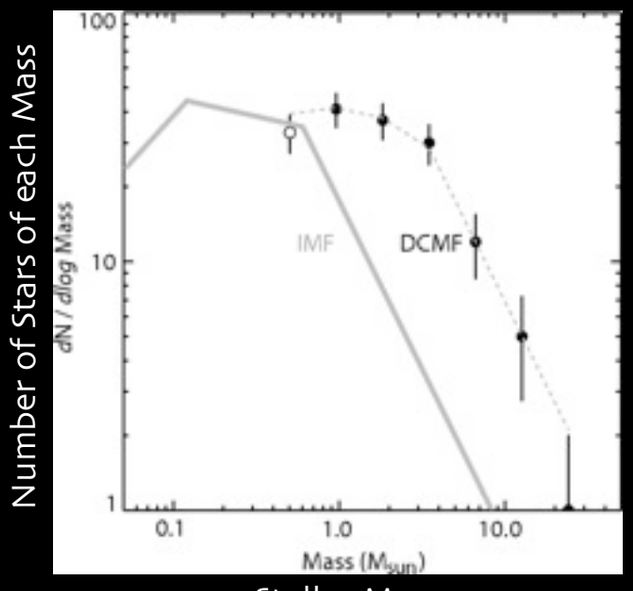

Stellar Mass

"IMF"? "CMF"?

Note: IMF= "Initial Mass Funciton" of Stars, not "International Monetary Fund."

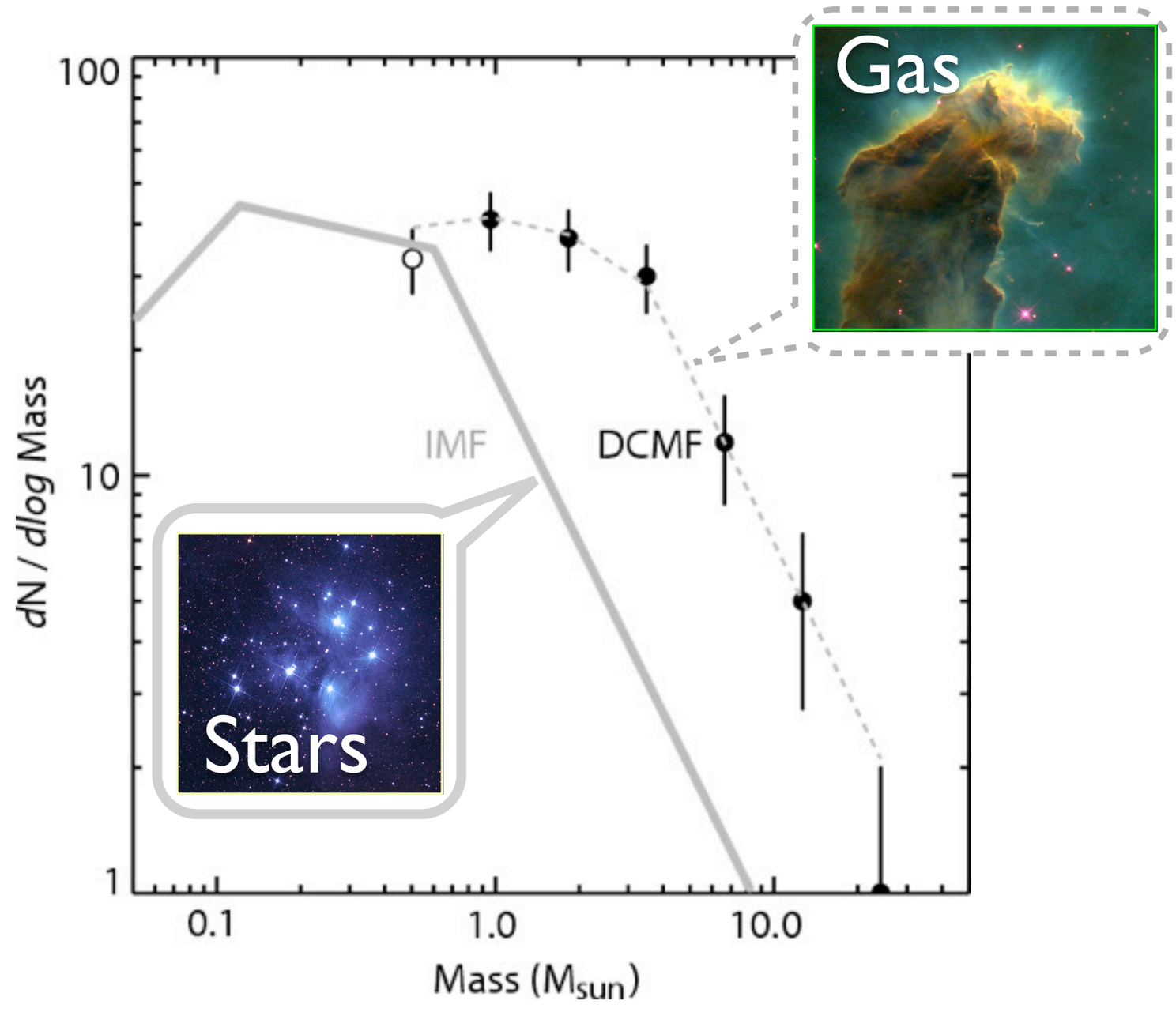

Alves, Lombardi & Lada 2007

BUT: Beautiful images like this do not reveal *internal* structure directly...

simulations

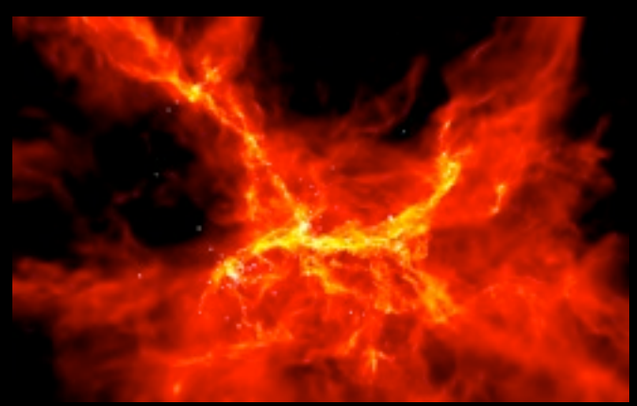

>2D observations

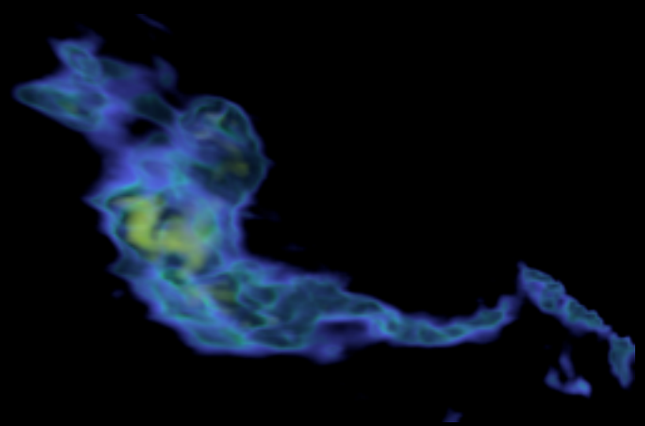

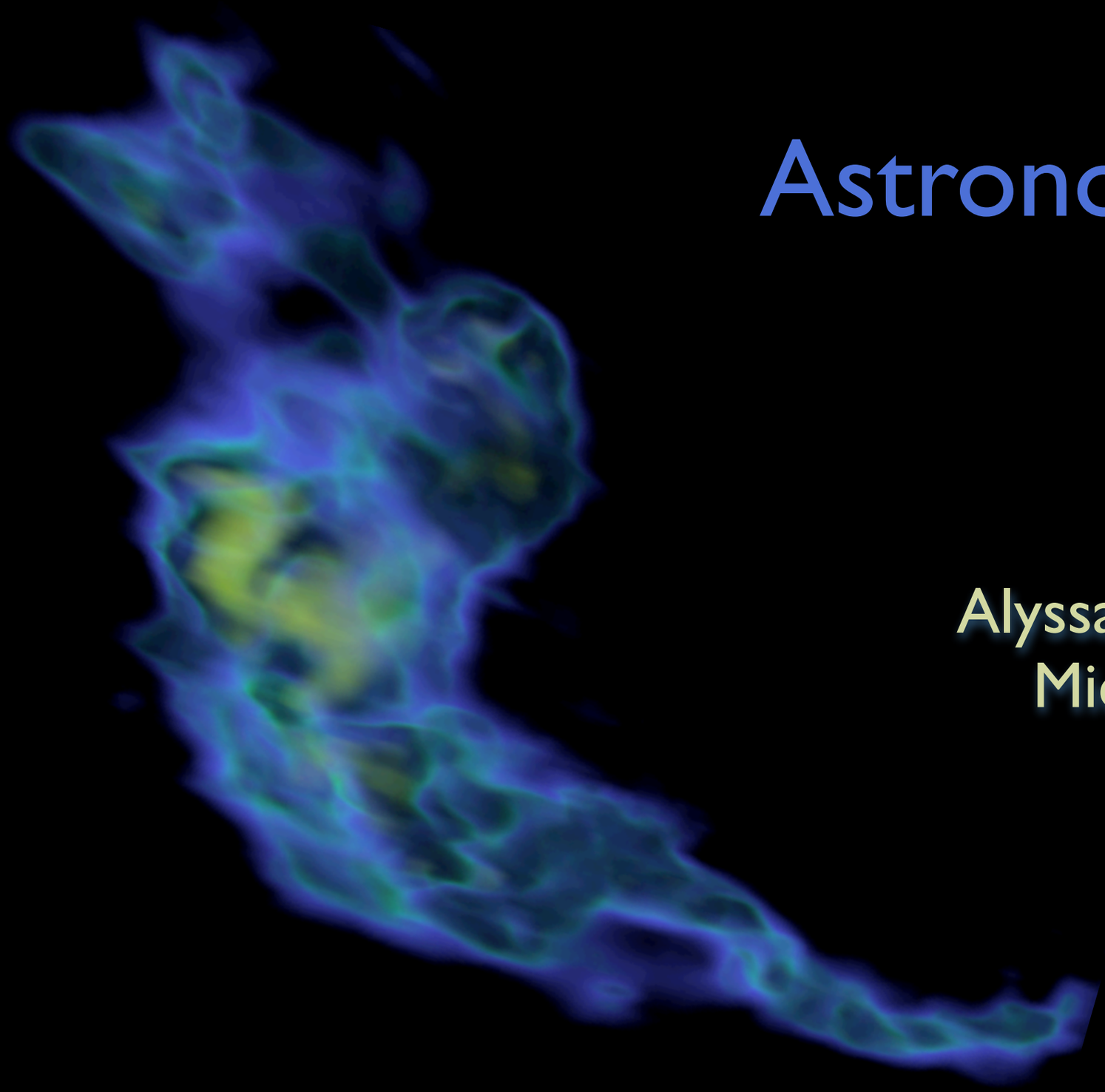

Astronomical Medicine

Alyssa Goodman (IIC/CfA/FAS)
Michael Halle (IIC/SPL/HMS)
Ron Kikinis (SPL/HMS)
Douglas Alan (IIC)
Michelle Borkin (FAS/IIC)
Jens Kauffmann (CfA/IIC)
Erik Rosolowsky (CfA/UBC Okanagan)
Nick Holliman (U. Durham)

The Astronomical Medicine Story

Computer Scientist

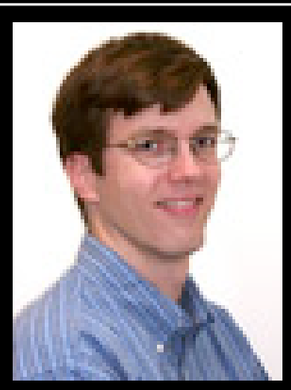

Computer Scientist

Unsuspecting Undergrad

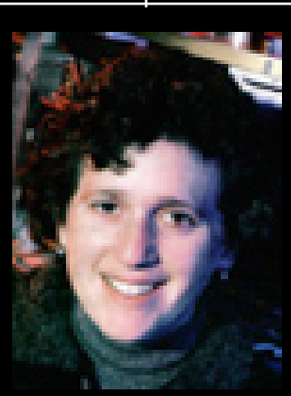

Astronomer

"Viz has failed the scientific community…"

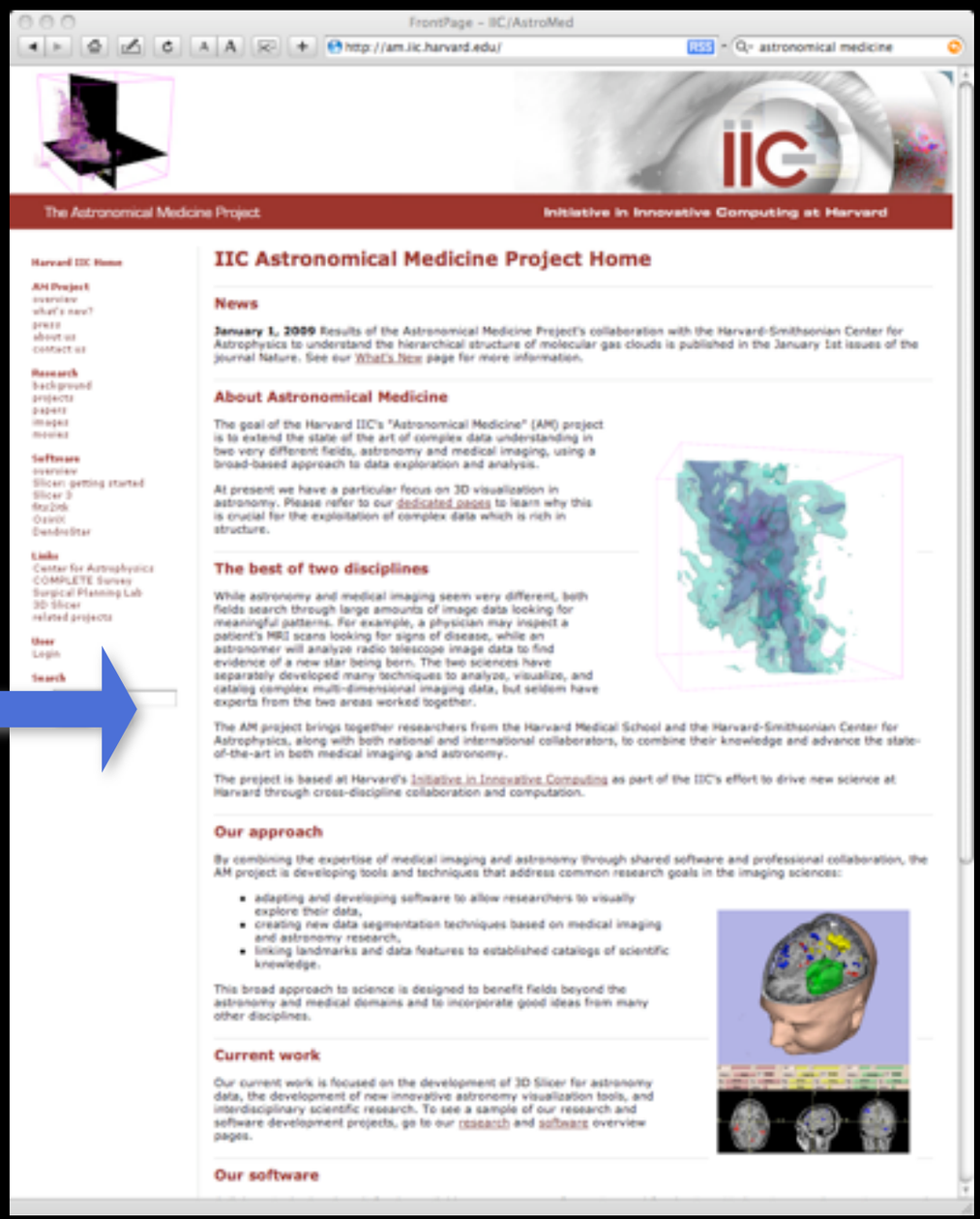

+Nick Holliman (CS, 3D expert)
+Doug Alan (S/W Engineer)
+Jens Kauffmann (postdoc)
+Erik Rosolowsky (postdoc) + ...

COMPLETE =**CO**ordinated **M**olecular **P**robe **L**ine **E**xinction **T**hermal **E**mission

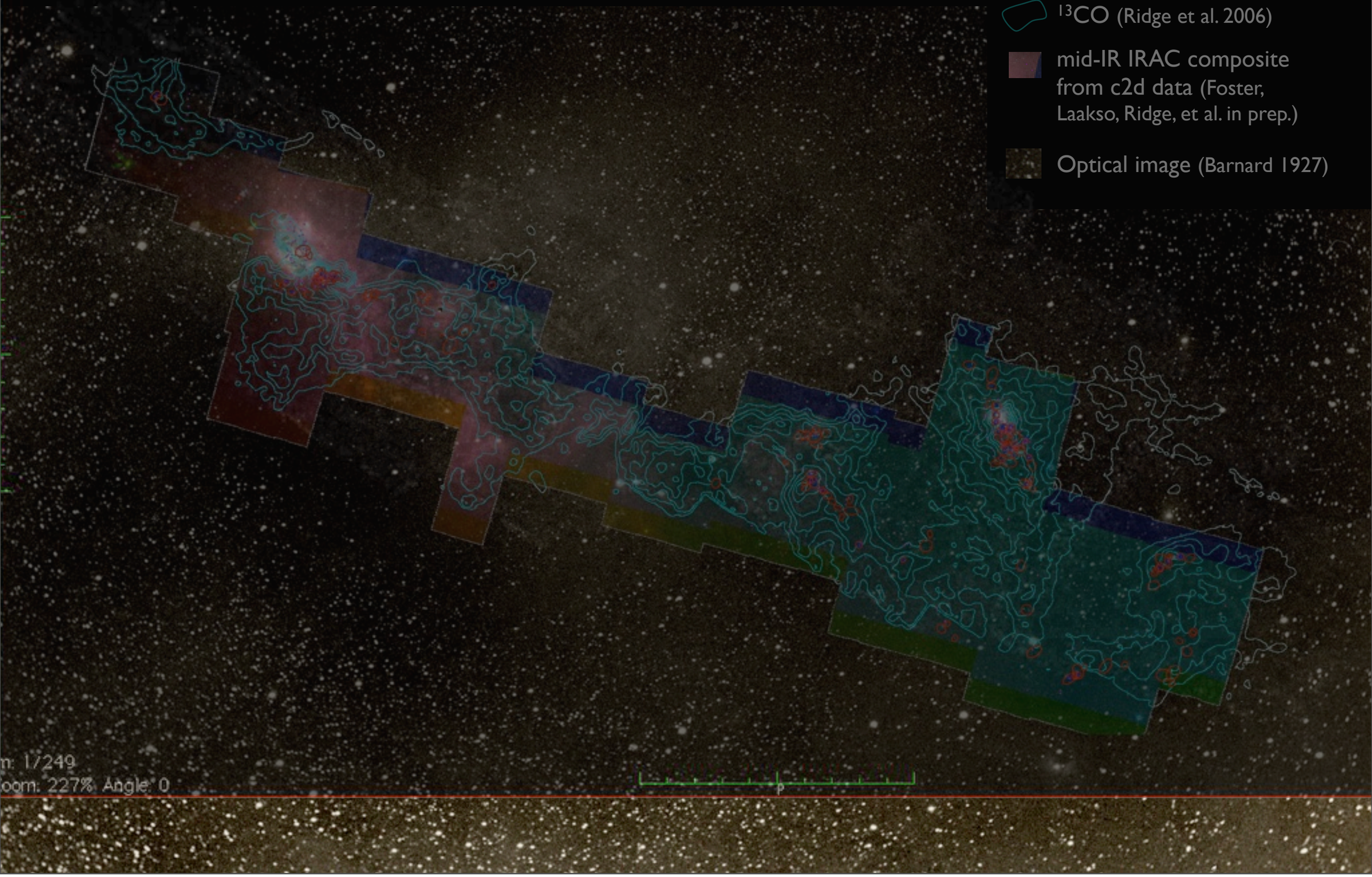

"Three" Dimensions: Spectral-Line Mapping

We wish we could measure…

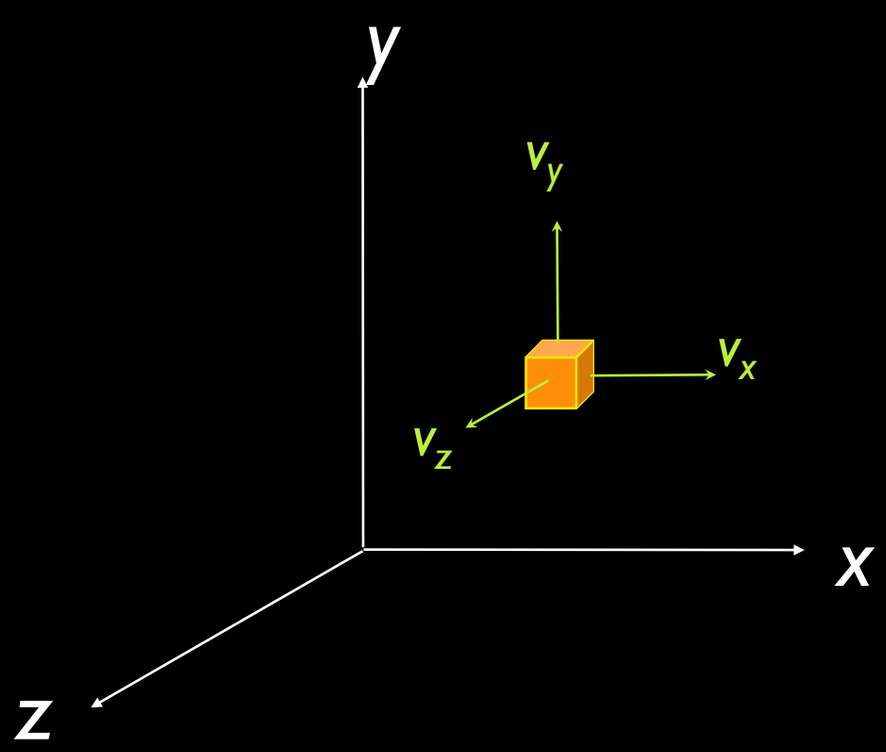

But we can measure…

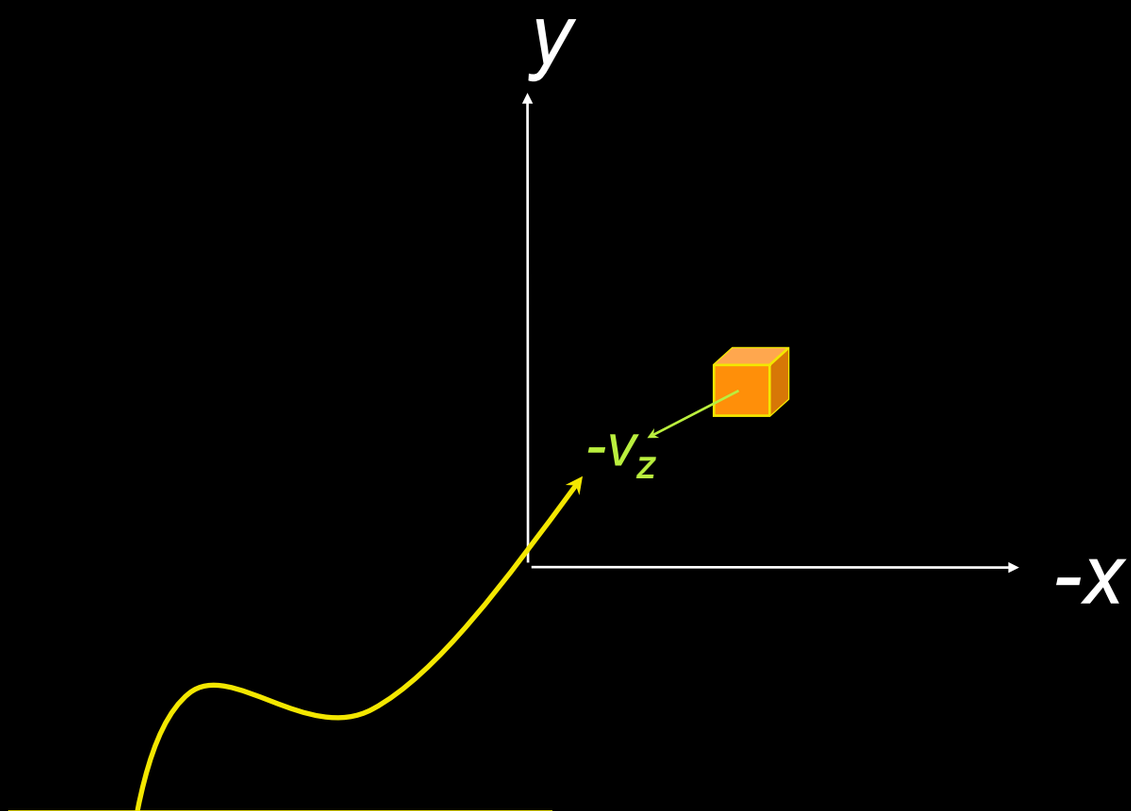

v_z *only* from "spectral-line maps"

Velocity from Spectroscopy

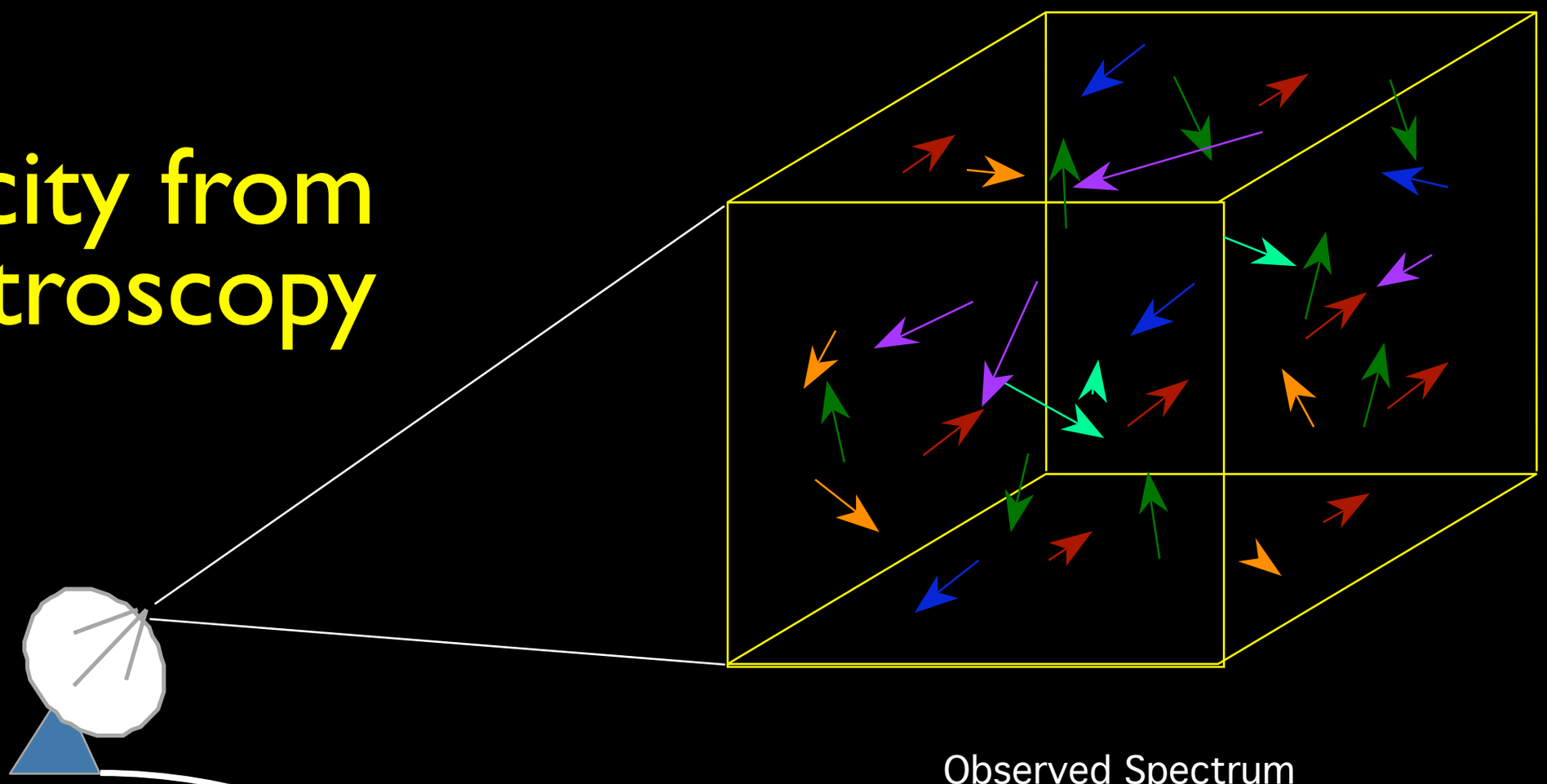

Telescope + Spectrometer

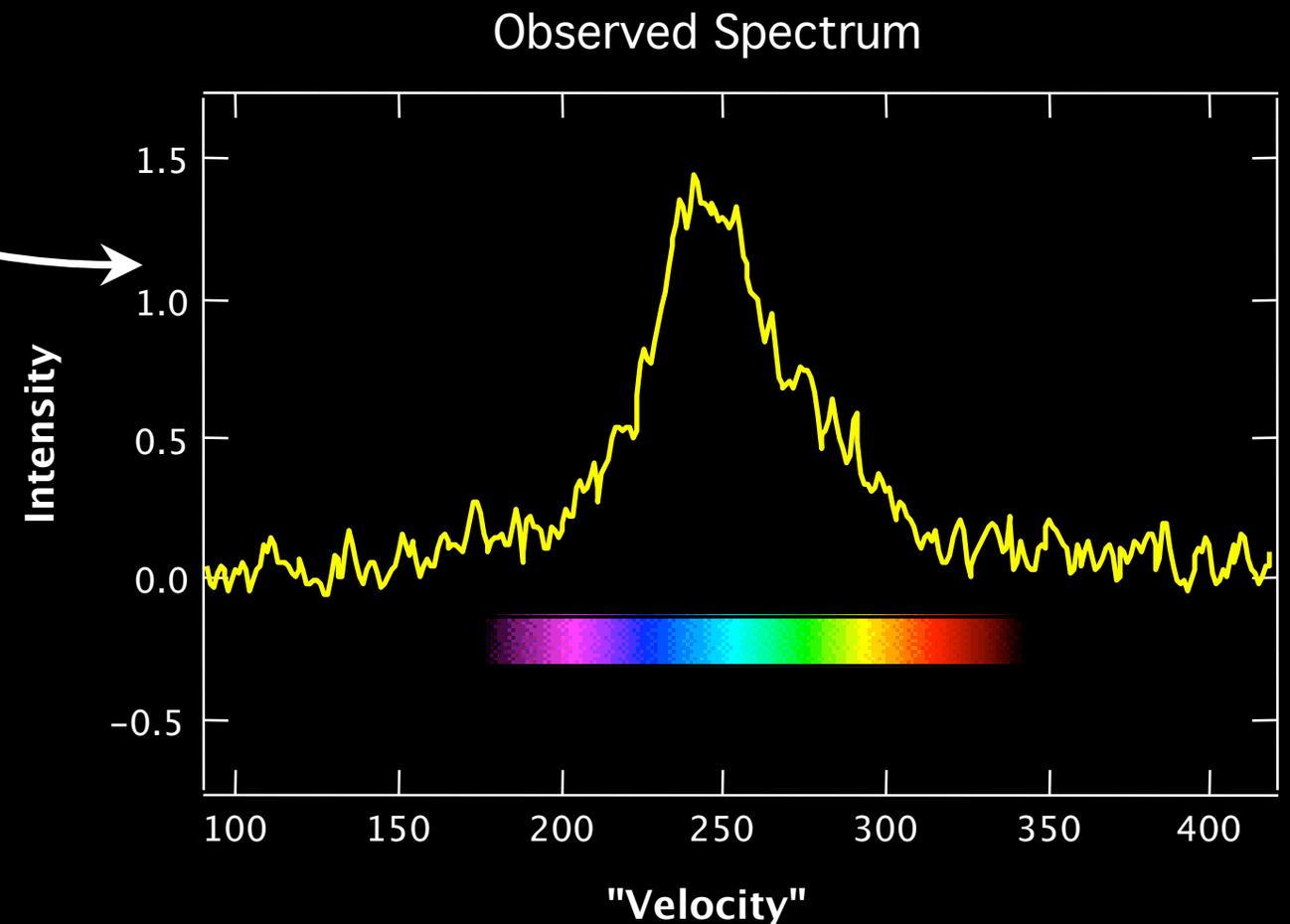

All thanks to Doppler

Radio Spectral-line Observations of Interstellar Clouds

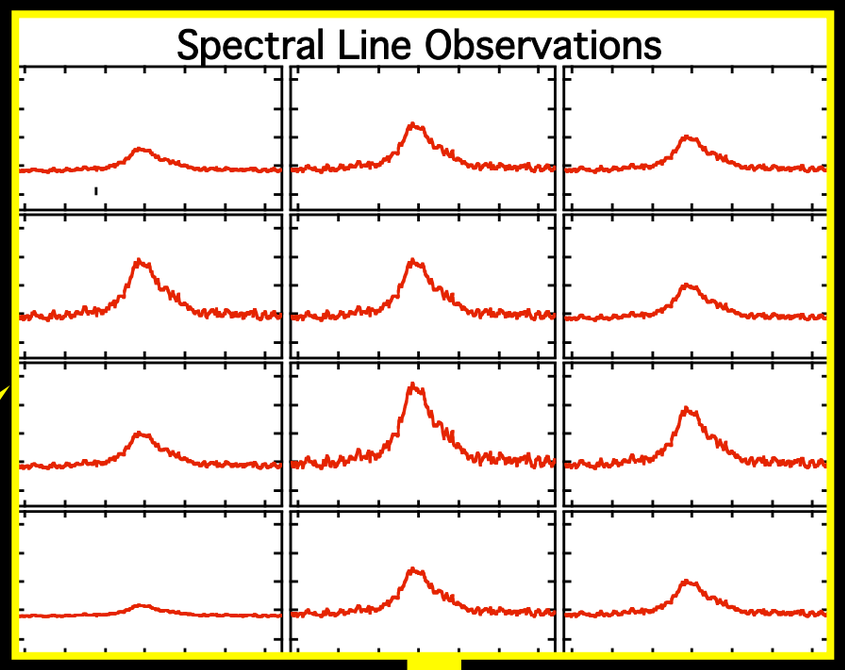

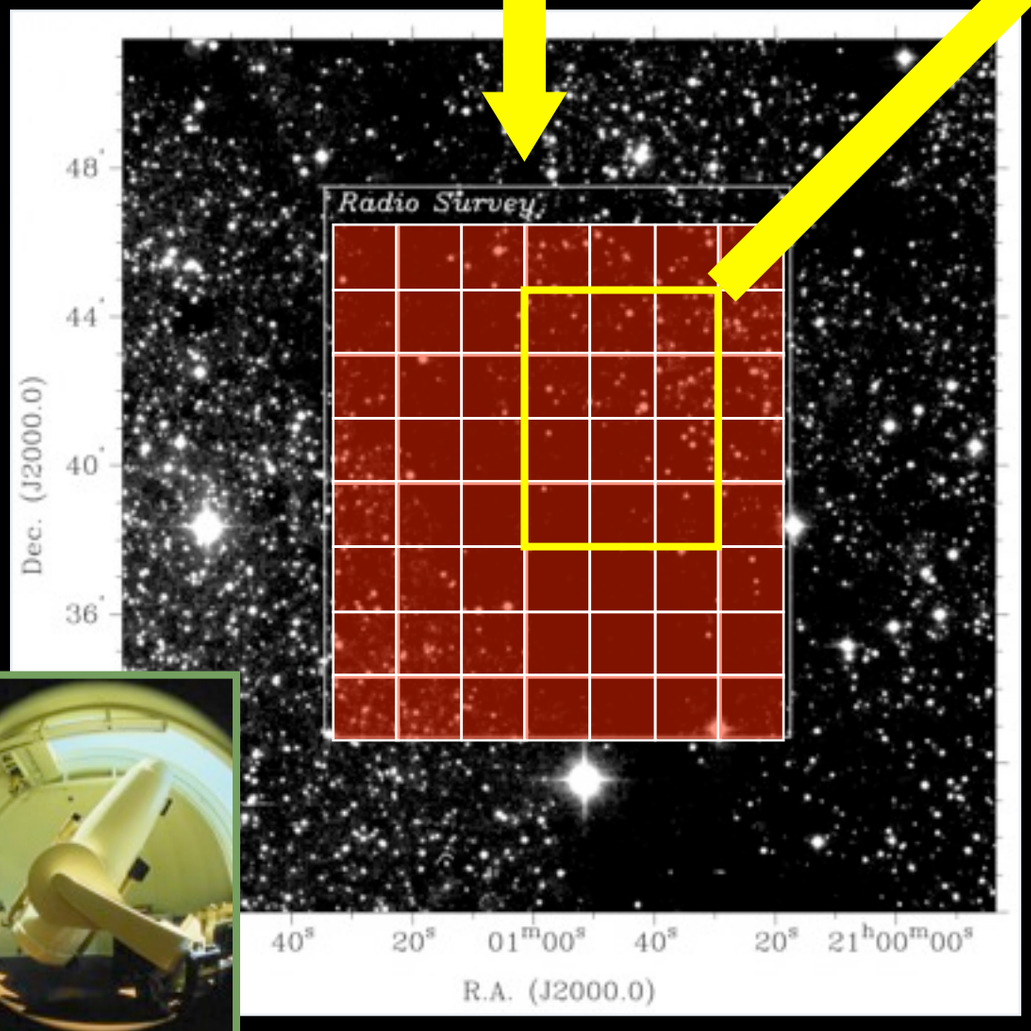

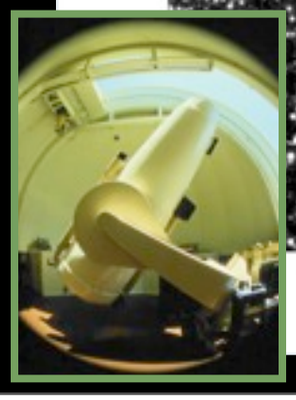

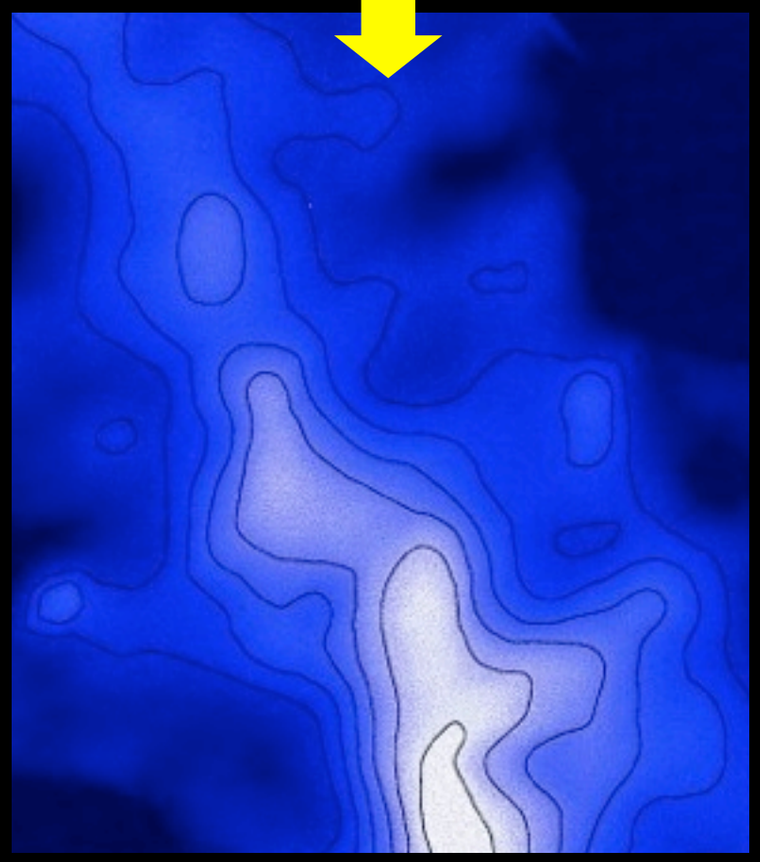

Radio Spectral-line Observations of Interstellar Clouds

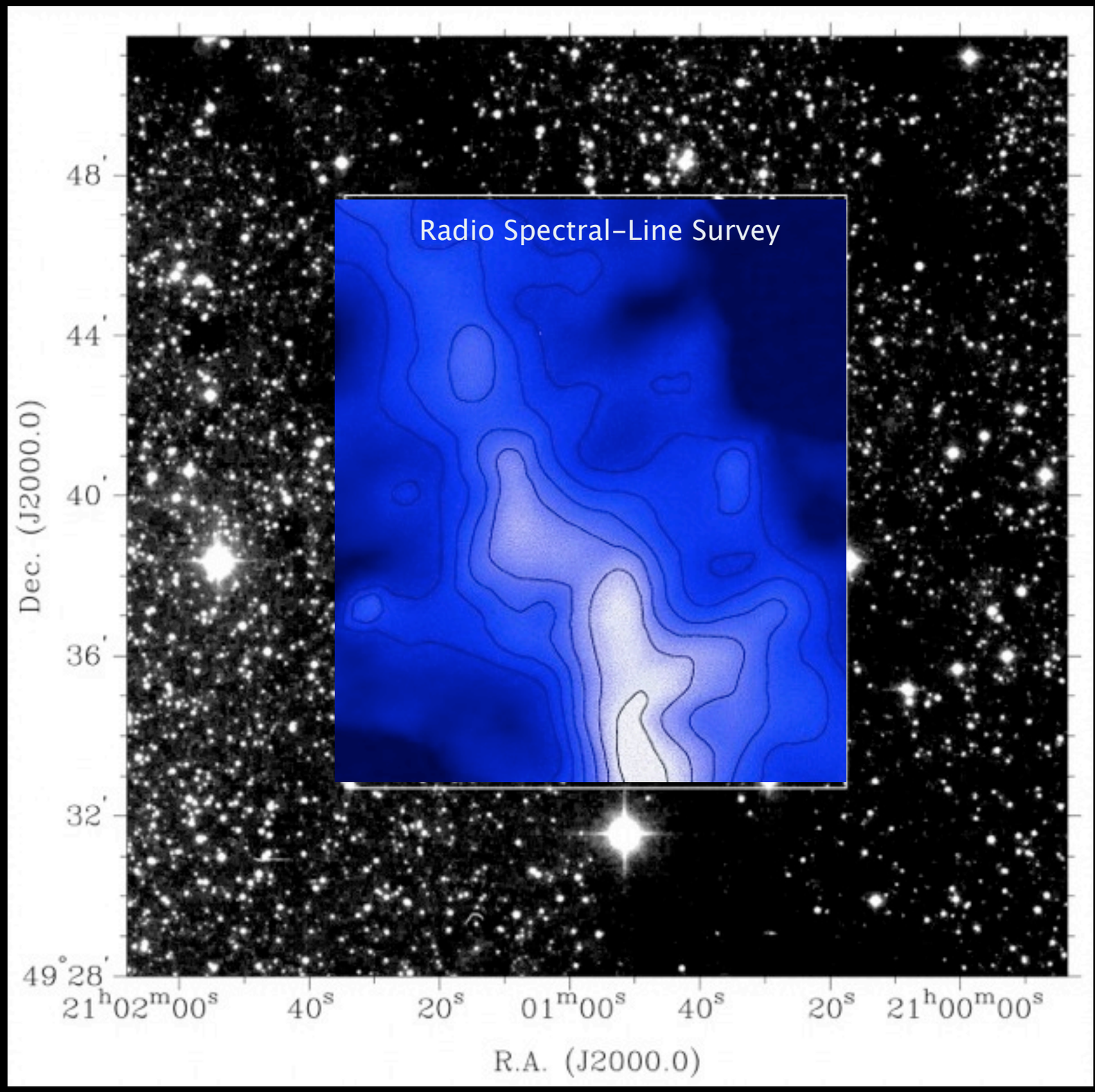

Alves, Lada & Lada 1999

Velocity as a "Fourth" Dimension

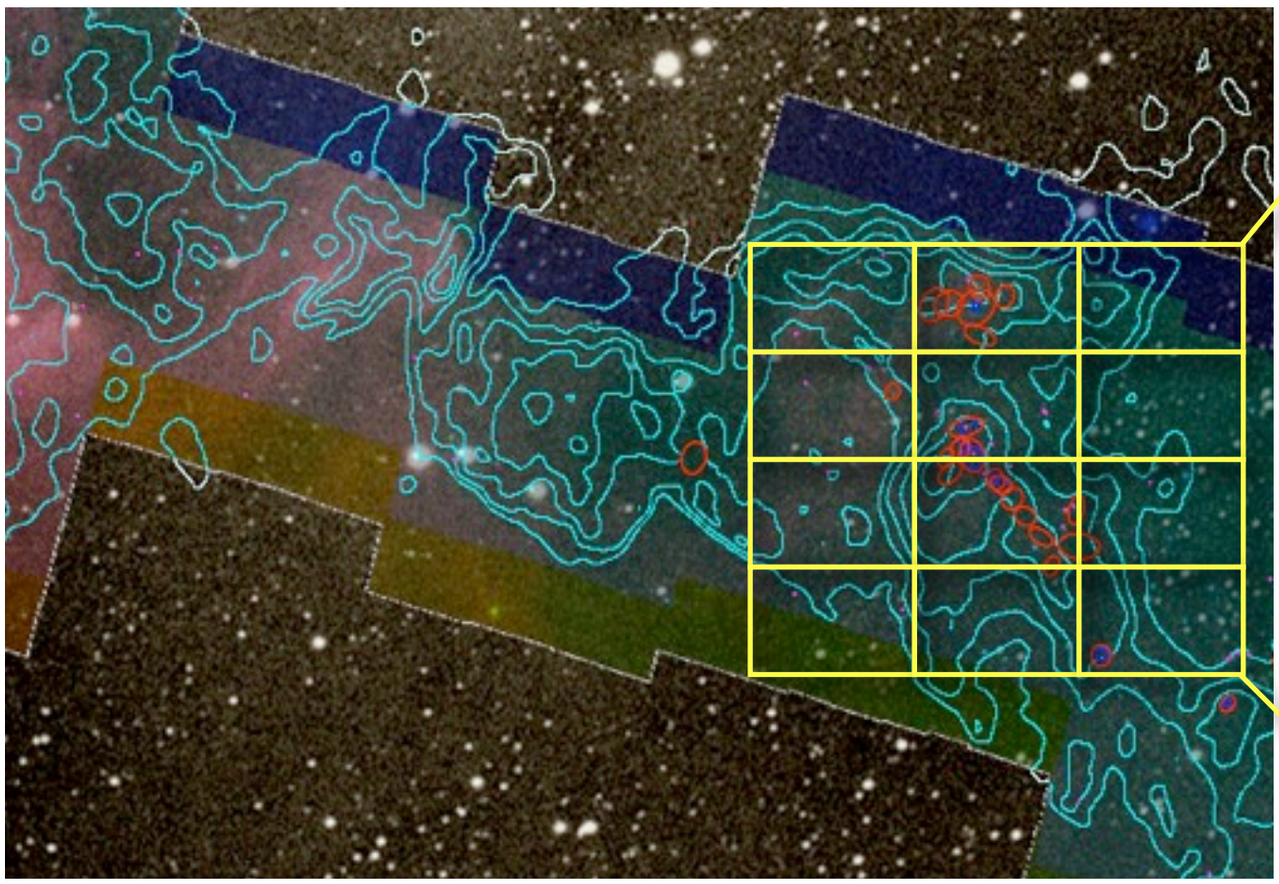

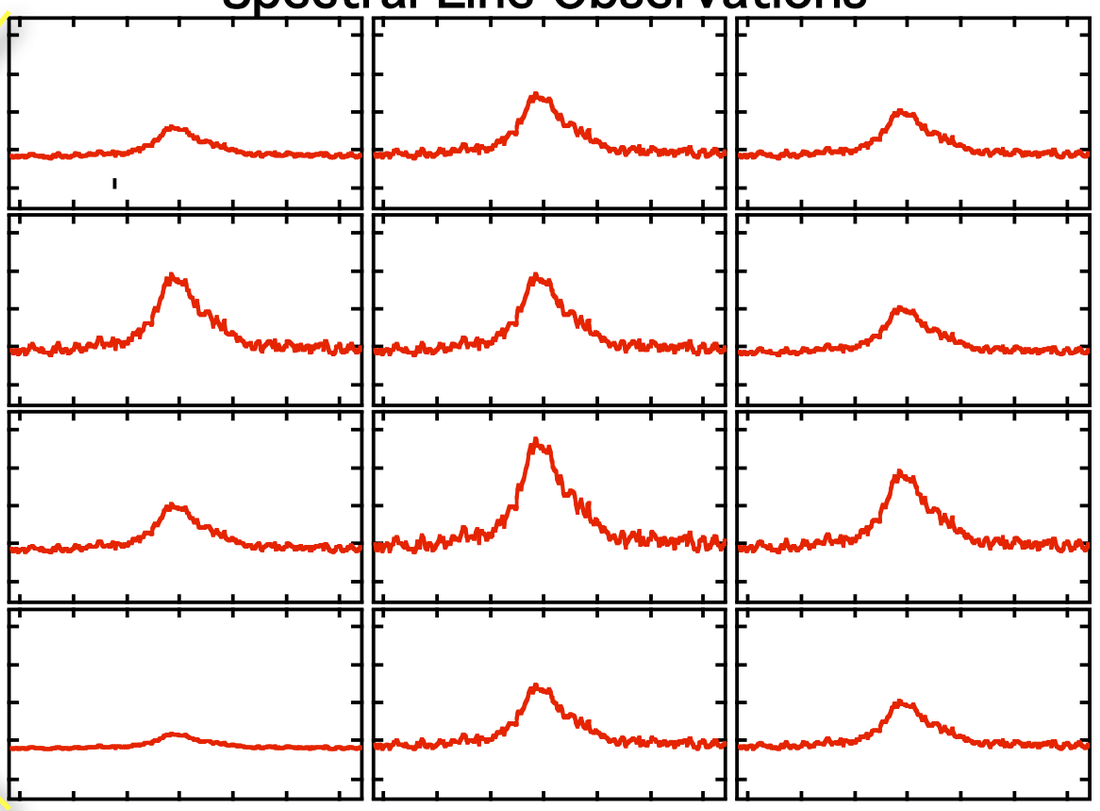

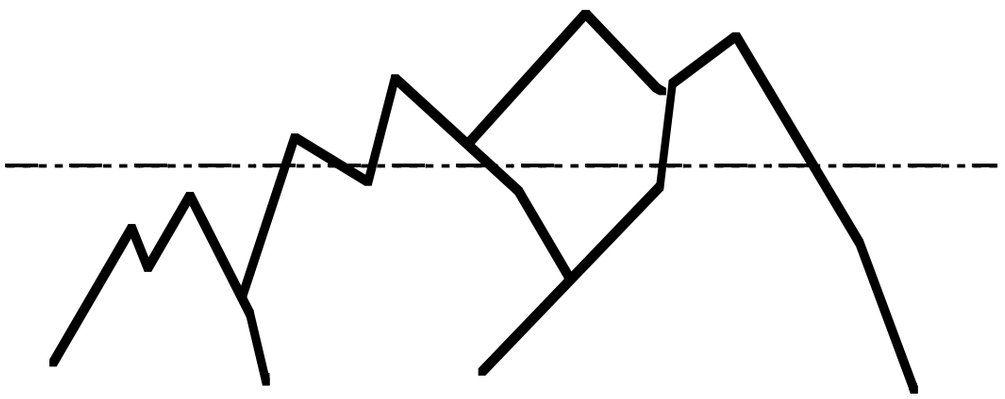

Mountain Range

No loss of information

Loss of 1 dimension

Astronomical Visualization Tools are Traditionally 2D

IDL

DS9

Karma*

GAIA

Aipsview

3D Slicer

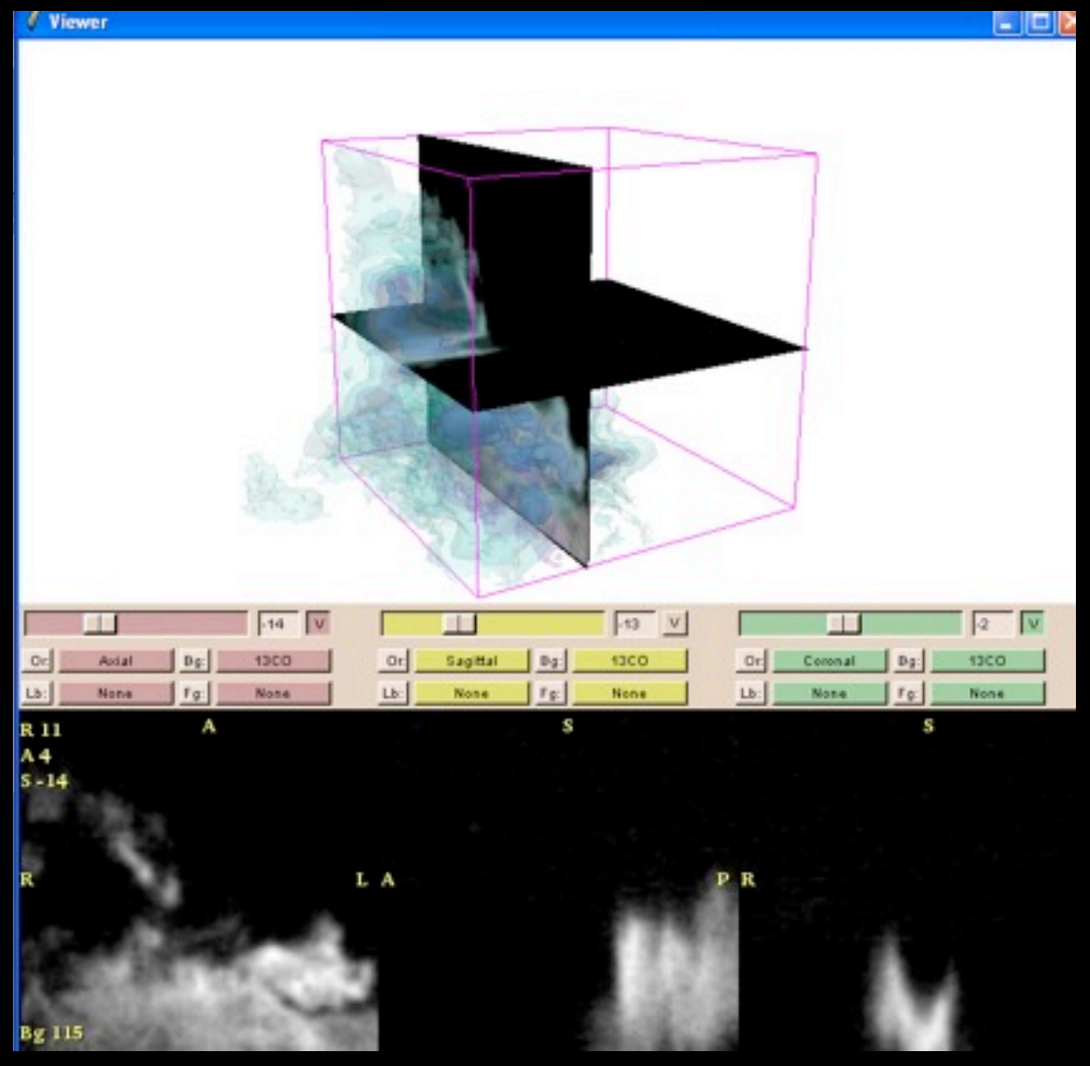

"3D"=movies

Challenge in displaying spectral line data cubes.

Hard to address all three dimensions at once, but made compact with 3D Slicer.

3D Slicer is a visualization tool taking fundamentally different approach.

3D Slicer built and designed for 3D viewing; others come from 2D approach.

"Astronomical Medicine"

"KEITH"

"PERSEUS"

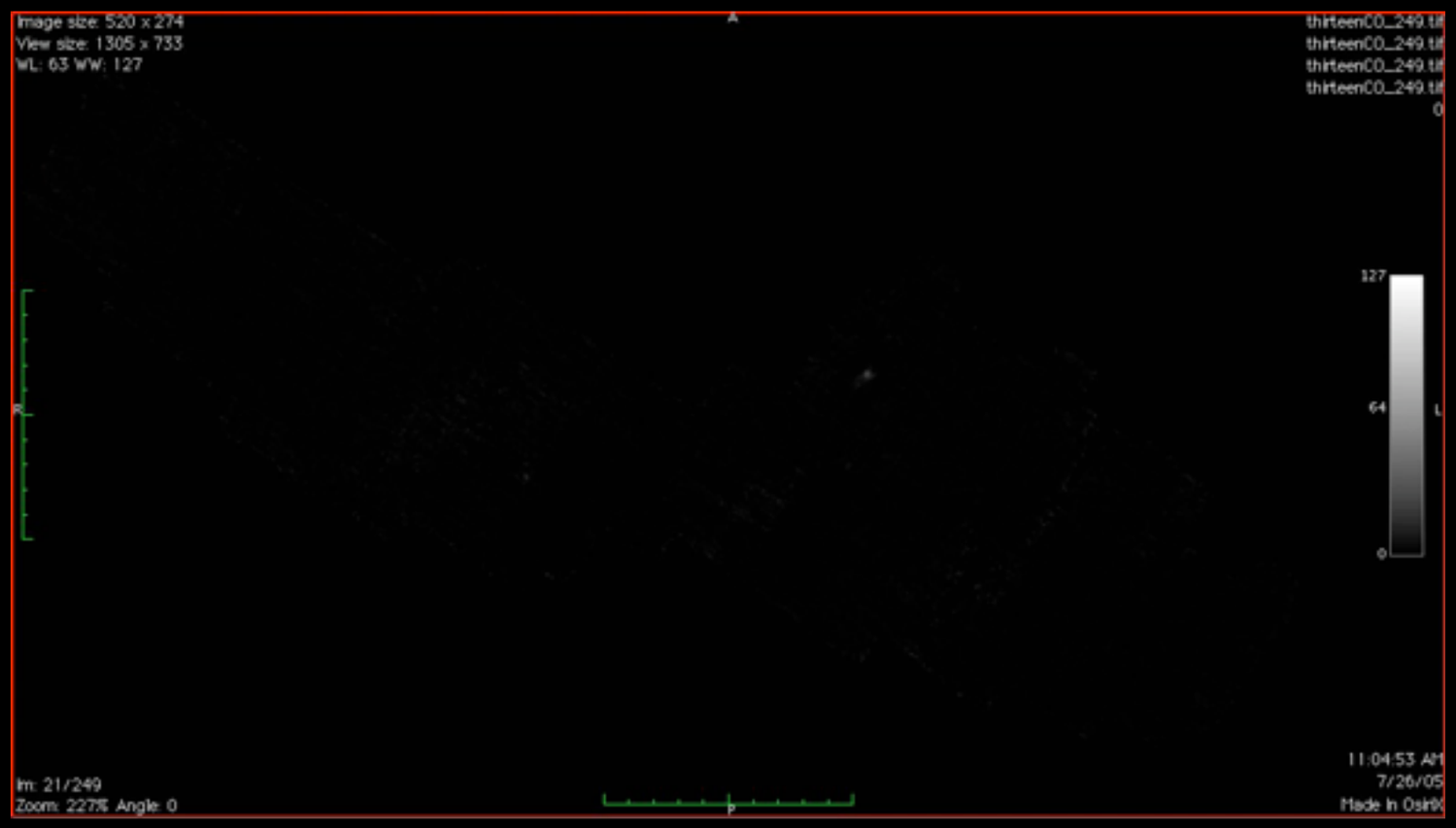

"z" is depth into head

"z" is line-of-sight velocity

(This kind of "series of 2D slices view" is known in the Viz as "the grand tour")

What can we observe?

$$I(E, s, \vec{x}, t)$$

Intensity

Energy
(wavelength)

“State”
(e.g. polarization)

Spatial Position
(x, y, z)

Time

...and the science is in the interpretation of these measurements into physical quantities & processes.

What can we observe?

$$I(\quad \vec{x} \quad)$$

Intensity

Spatial Position

$(x, y \quad)$

Optical Single-Band
Image of NGC1333

What can we observe?

$$I(\quad \vec{x} \quad)$$

Intensity

Spatial Position

$$(x, y \quad)$$

X-Ray of Human Skull, c. 1920

What can we observe?

$$I(\quad \vec{x}, t)$$

Intensity

Time

Spatial Position

(x, y, z)

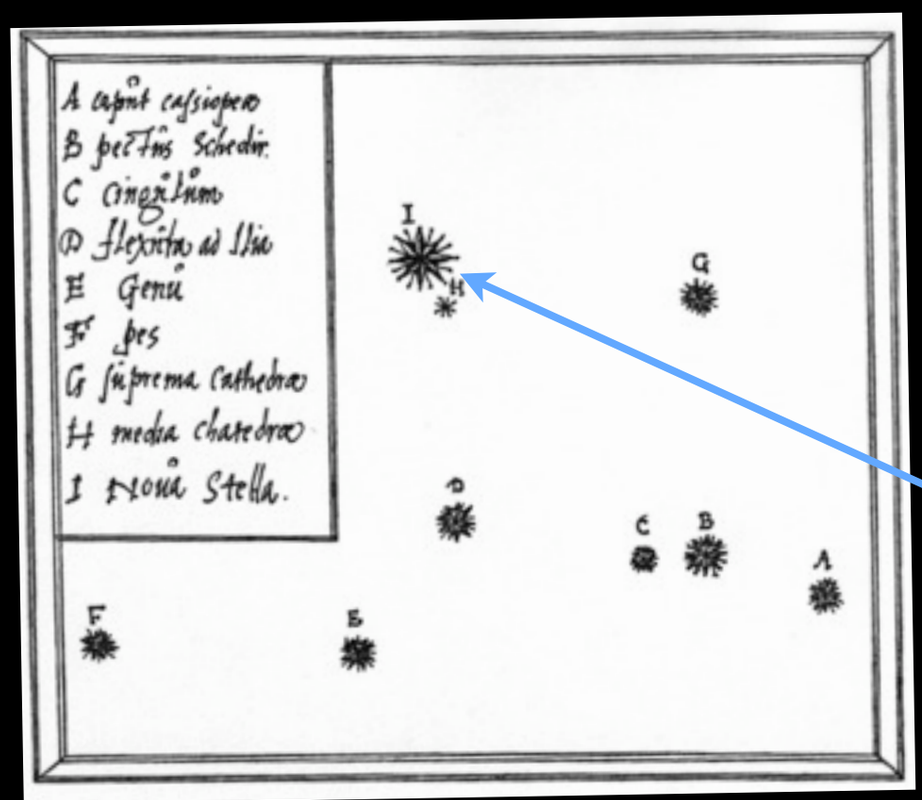

"Nova Stella"
of Tycho, 1572

What can we observe?

$$I(\quad\quad\quad \vec{x}, t)$$

Intensity

Time

Spatial Position
(x, y, z)

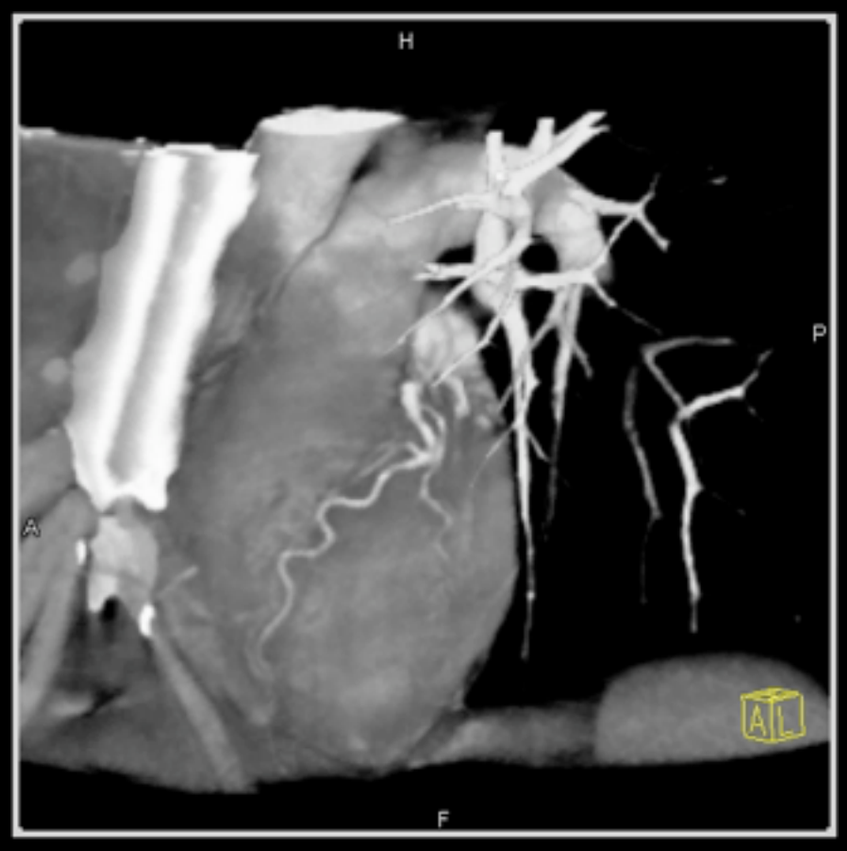

Cardiac Motion

Monday, November 16, 2009

Cardiac Motion: This is an excellent demonstration of why we need to reconstruct at various sequences in the cardiac cycle. You will note how depending on the contracting heart, the right coronary artery is either absolutely normal or evaluation might be considered limited by motion related artifact. This is why we reconstruct all cases at 10% intervals. From: http://www.ctisus.org/rsna_2006/cardiac_cta/videos.html

What can we observe?

$$I(E, \quad \vec{x} \quad)$$

Intensity

Energy
(wavelength)

Spatial Position
$(x, y \quad)$

Optical (B,V,R) image
of NGC1333

What can we observe?

$$I(E, \quad \vec{x} \quad)$$

Intensity

Energy
(wavelength)

Spatial Position
$(x, y \quad)$

Human Ear,
Thermal Infrared

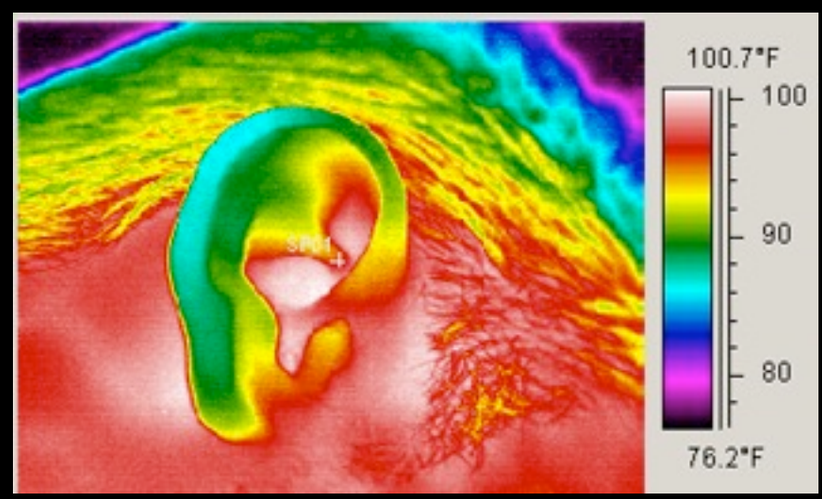

What can we observe?

$$I(\quad s, \vec{x} \quad)$$

Intensity

Spatial Position
$(x, y \quad)$

"State"
(e.g. polarization)

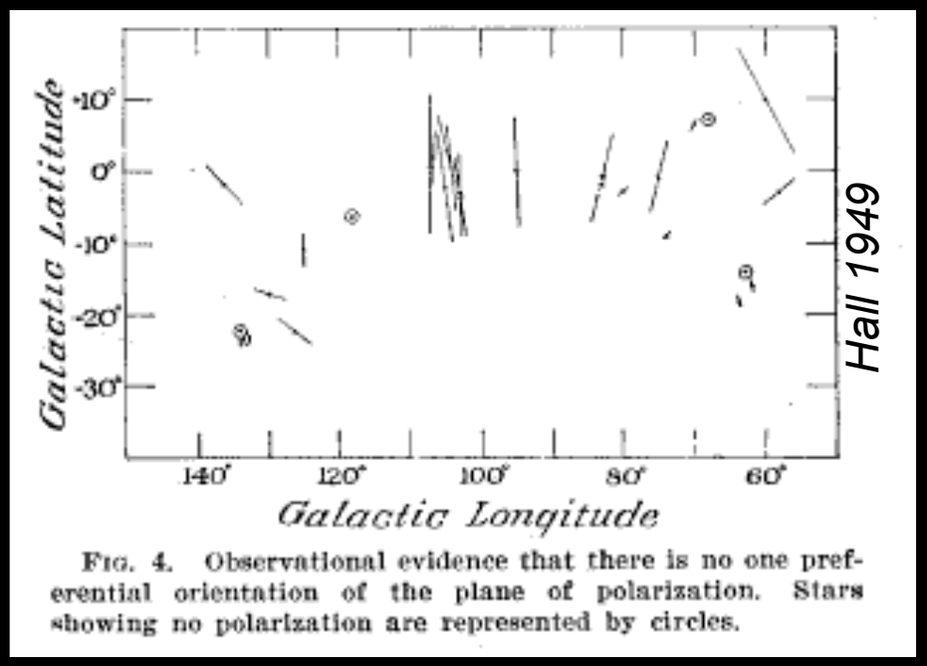

FIG. 4. Observational evidence that there is no one preferential orientation of the plane of polarization. Stars showing no polarization are represented by circles.

What can we observe?

$$I(\quad s, \vec{x} \quad)$$

Intensity

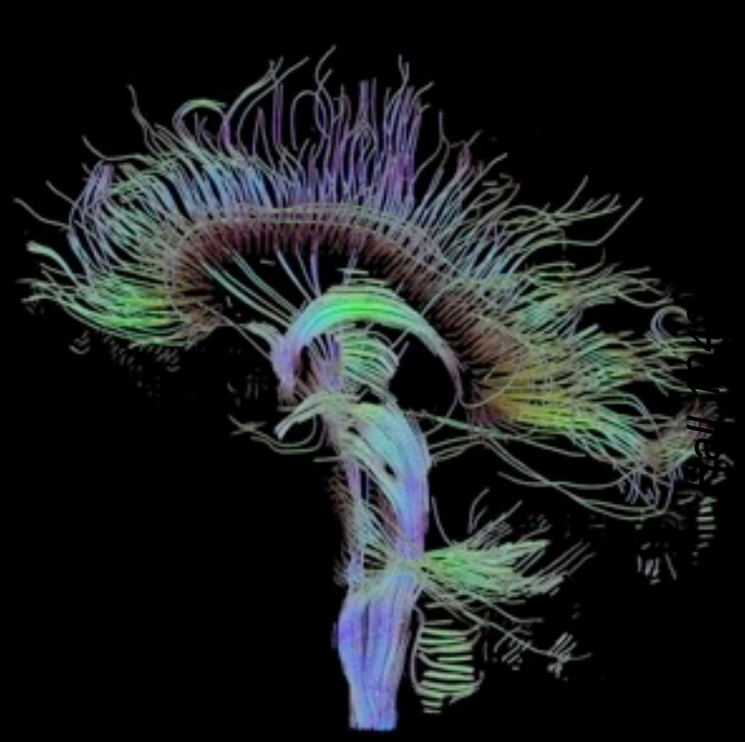

“State”
(~diffusivity)

Spatial Position
(x, y, z)

COMPLETE Perseus

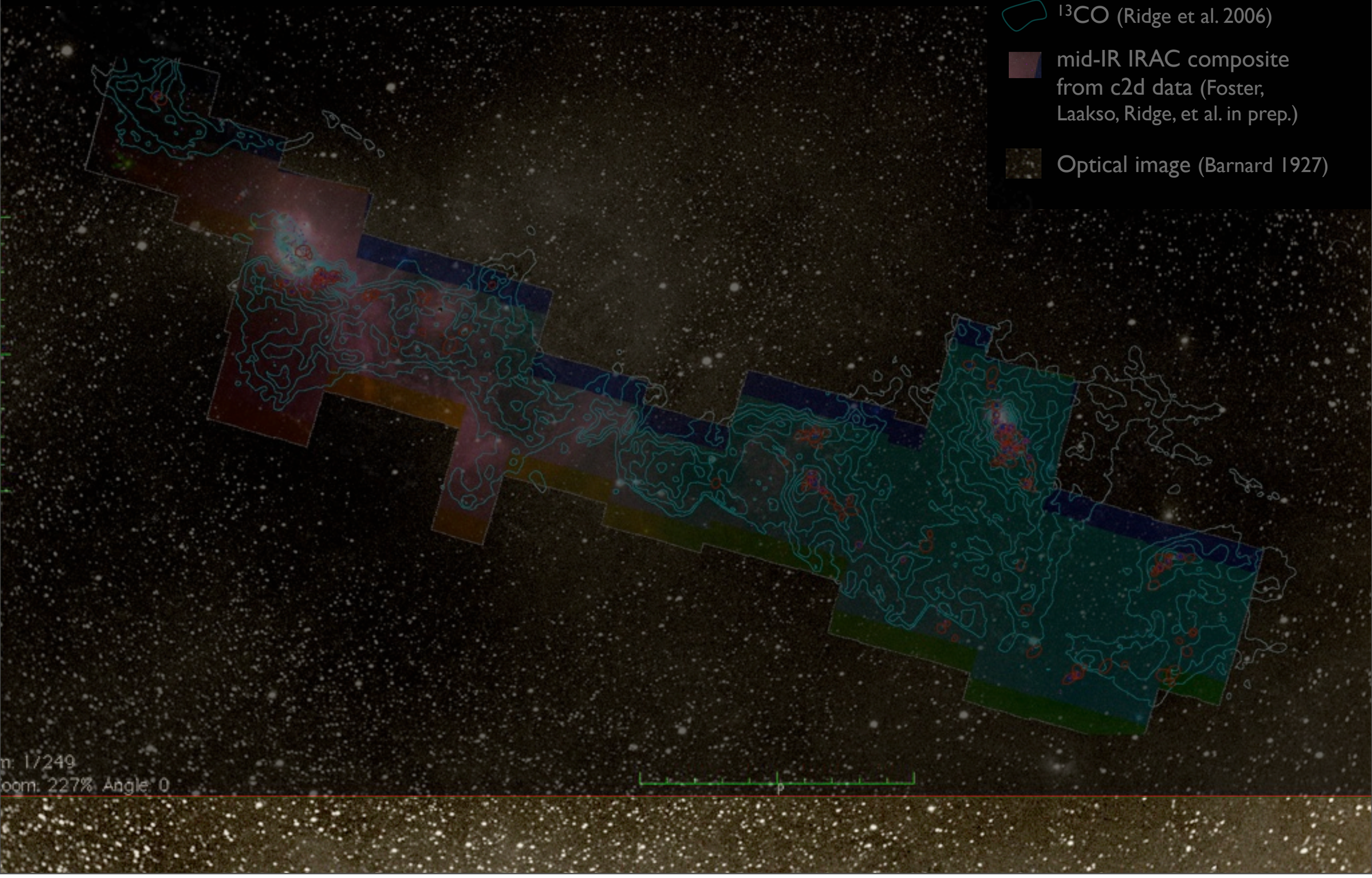

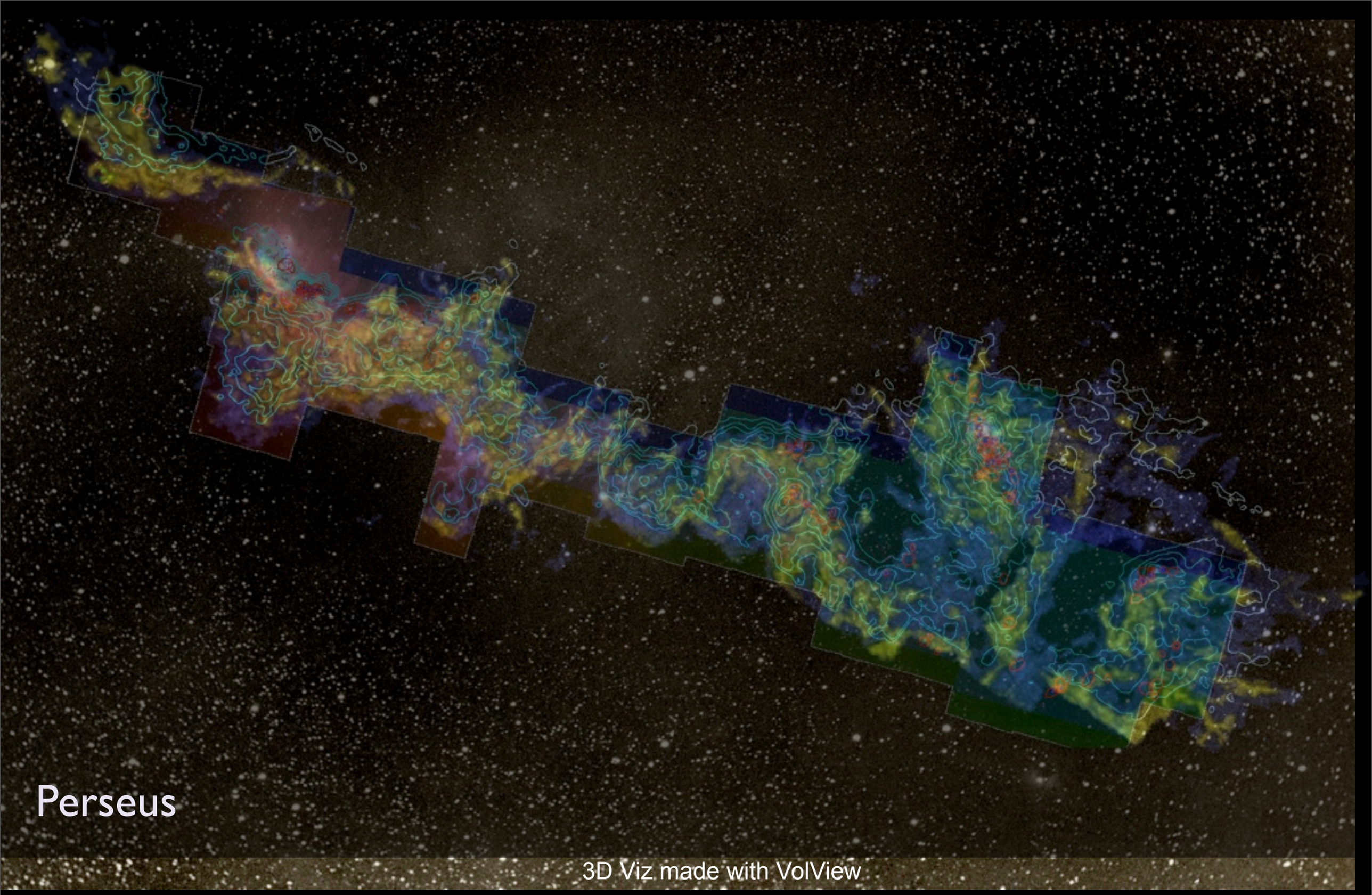

AstronomicalMedicine@IIG COMPLETE

Real 3D space

3D rendering: GE Healthcare

"Position-Position-Velocity" Space

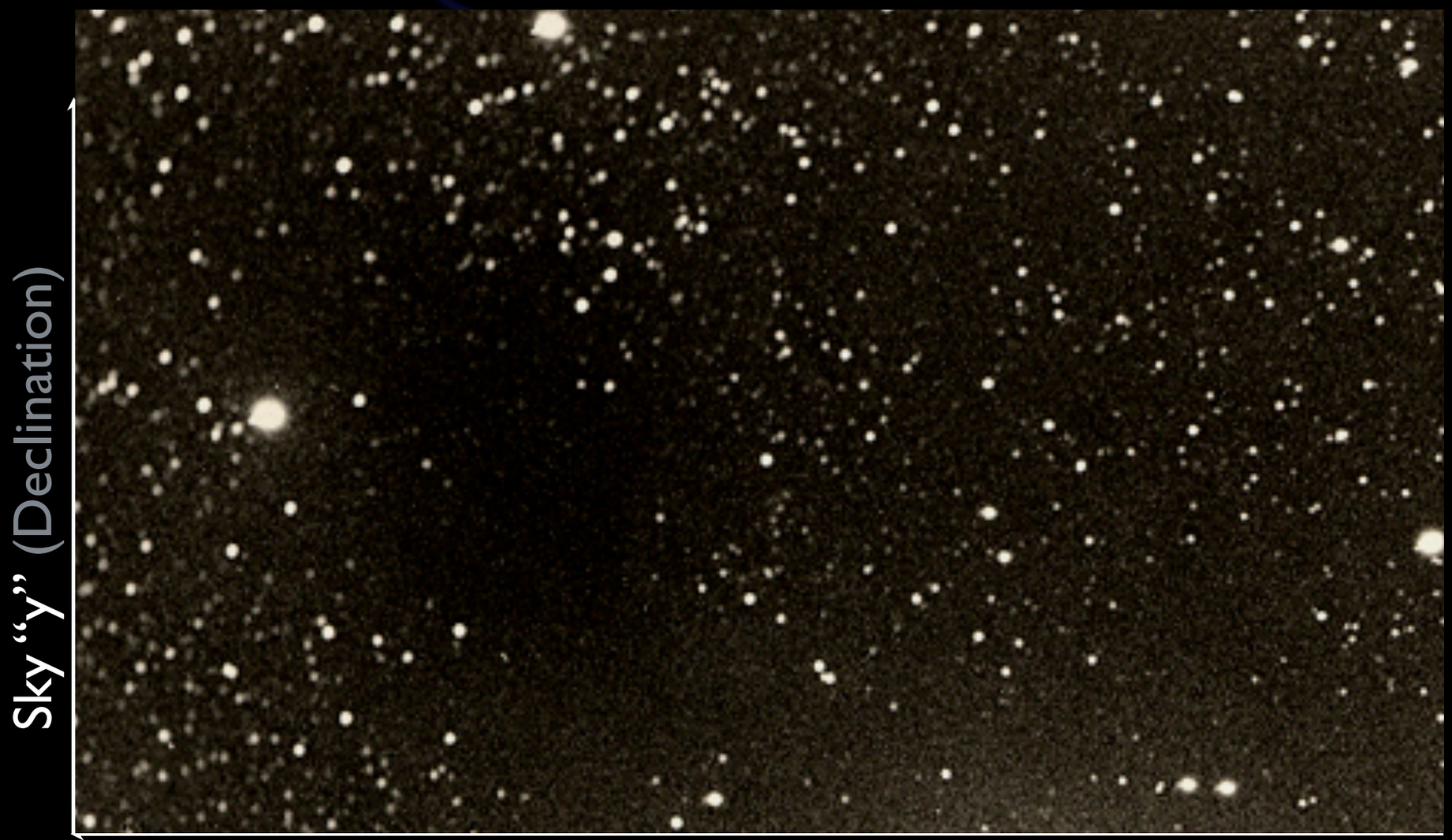

Sky "y" (Declination)

Sky "x" (Right Ascension)

3D rendering: AstroMed /N. Holliman (U. Durham), using VolView (ITK-based)

Some of What We've Learned...

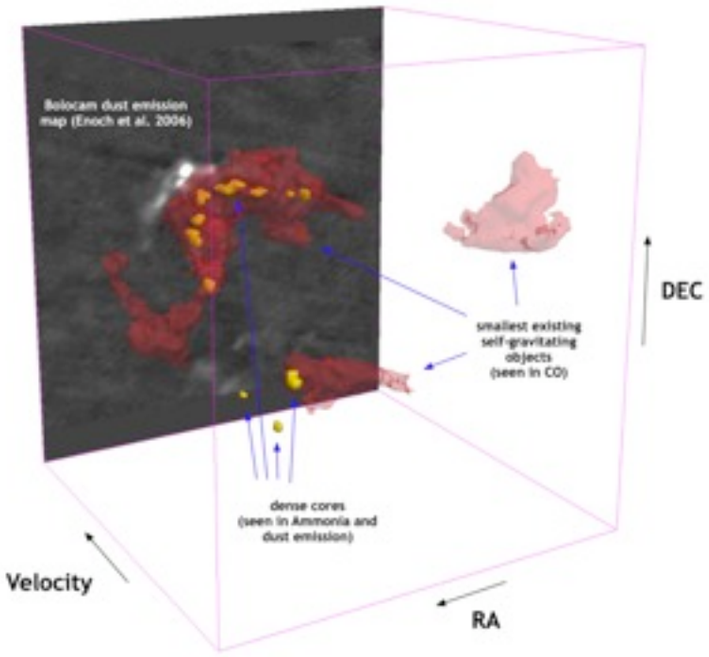

Cores nest in coccoons (Kauffmann et al. 2009)

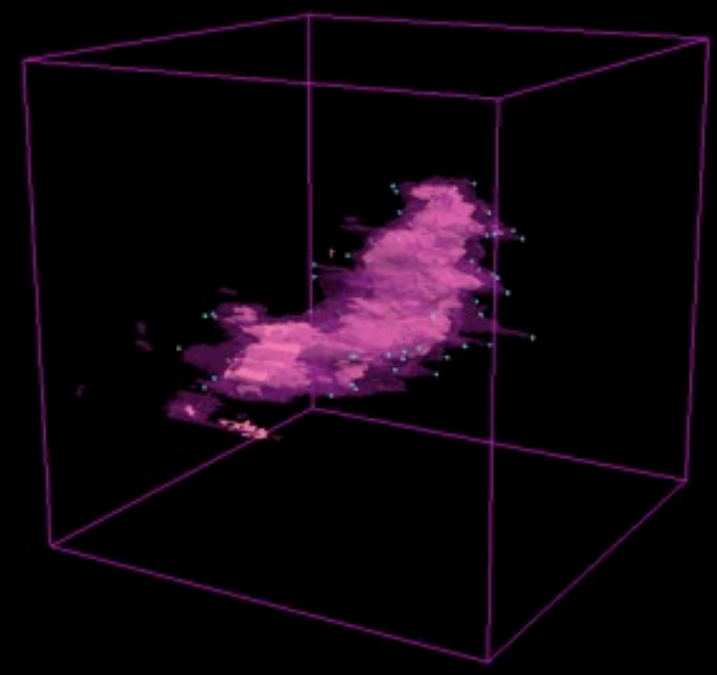

Tripled Outflows (Borkin et al. 2008,9)

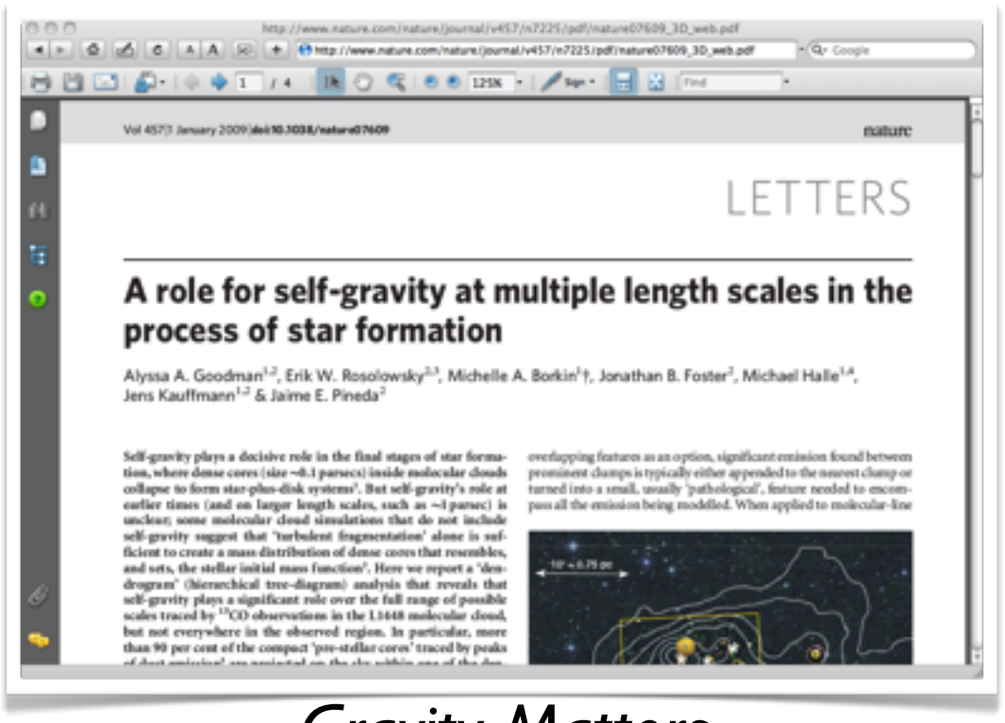

Gravity Matters (Goodman et al. 2009)

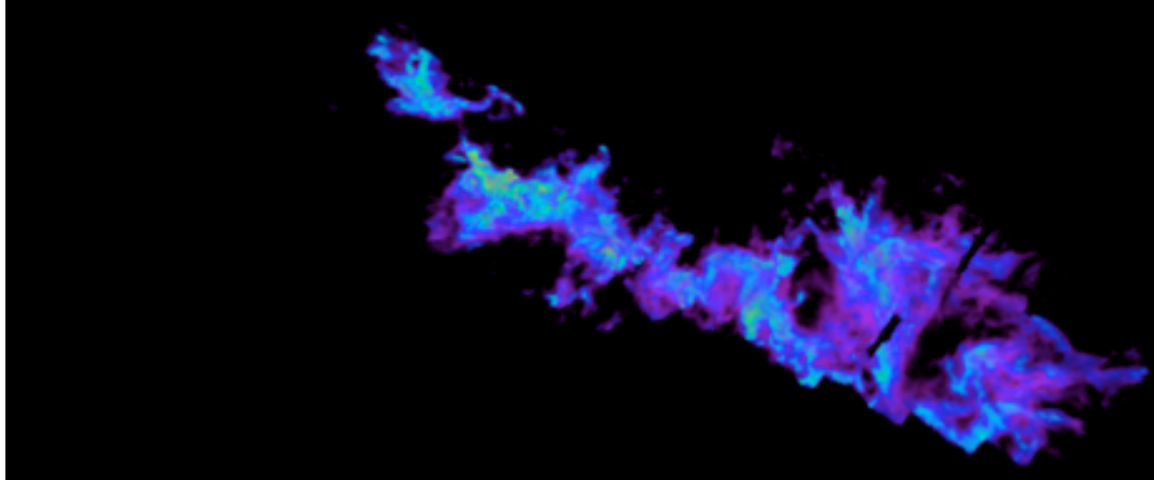

Shells Rule (Arce et al. 2009)

Astronomical

The Publication Database hosted by SPL

All Publications | Upload | Advanced Search | Gallery View | Download Statistics | Help | Import | Log in

Search

A role for self-gravity at multiple length scales in the process of star formation

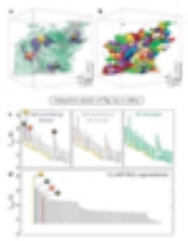

[1]Alyssa A Goodman, [2]Erik W Rosolowsky, [1]Michelle A Borkin, [2]Jonathan B Foster, [1]Michael Halle, [1]Jens Kauffmann, [2]Jaime E Pineda

Institution: [1]Initiative in Innovative Computing at Harvard, Cambridge, Massachusetts 02138, USA. agoodman@cfa.harvard.edu
[2]Harvard-Smithsonian Center for Astrophysics, Cambridge, Massachusetts 02138, USA.
Publisher: Nature
Publication Date: Jan-2009
Citation: Nature. 2009 Jan 1;457(7225):63-6.
PubMed ID: 19122636
Appears in Collections: NA-MIC, SLICER, SPL
Sponsors: U54 EB005149 (EB) funded by NIBIB NIH HHS
Generated Citation: Goodman A, Rosolowsky E, Borkin M, Foster J, Halle M, Kauffmann J, Pineda J. A role for self-gravity at multiple length scales in the process of star formation. Nature. 2009 Jan 1;457(7225):63-6. PMID: 19122636.
Downloaded: 376 times. [view map]
Paper: Download, View online

Medicine

The Publication Database hosted by SPL

All Publications | Upload | Advanced Search | Gallery View | Download Statistics | Help | Import | Log in

Search

A Mathematical Framework for Incorporating Anatomical Knowledge in DT-MRI Analysis

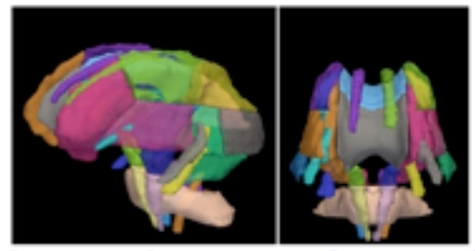

[1]Mahnaz Maddah, [1]Lilla Zollei, [1]W E L Grimson, [2]C-F Westin, [3]William M Wells III

Institution: [1]Computer Science and Artificial Intelligence Laboratory, Massachusetts Institute of Technology, Cambridge, MA, USA.
[2]Laboratory of Mathematics in Imaging, Brigham and Women's Hospital, Harvard Medical School, Boston, MA, USA.
[3] Surgical Planning Lab, Department of Radiology, Brigham and Women's Hospital, Boston, MA, USA.
Publisher: IEEE Symposium on Biomedical Imaging ISBI
Publication Date: May-2008
Citation: Proceedings of the 5th IEEE International Symposium on Biomedical Imaging: From Nano to Macro 2008; 4543943: 105–108.
PubMed ID: 19212449
PMCID: PMC2638065
Keywords: Diffusion Tensor MRI, Clustering, Anatomical Information, Tract-Oriented Quantitative Analysis, Projects:DTIModeling
Appears in Collections: SPL, LMI, NA-MIC, NAC, NCIGT, SLICER
Sponsors: P41 RR13218-09/NCRR NIH HHS

Moving Science

[The Role Self-Gravity in Star Formation]

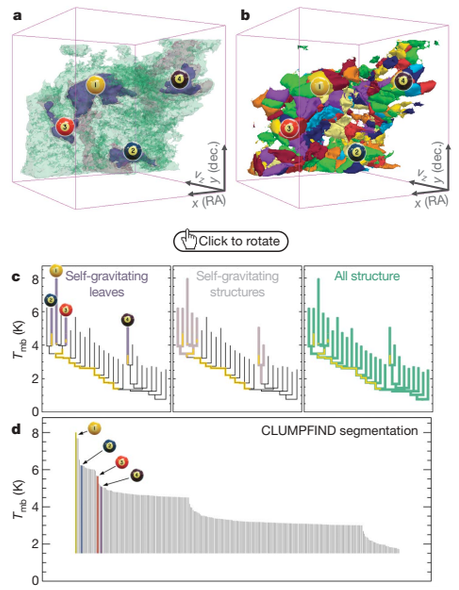

Figure 2 | Comparison of the 'dendrogram' and 'CLUMPFIND' feature-identification algorithms as applied to ^{13}CO emission from the L1448 region of Perseus. a, 3D visualization of the surfaces indicated by colours in the dendrogram shown in **c**. Purple illustrates the smallest scale self-gravitating structures in the region corresponding to the leaves of the dendrogram; pink shows the smallest surfaces that contain distinct self-gravitating leaves within them; and green corresponds to the surface in the data cube containing all the significant emission. Dendrogram branches corresponding to self-gravitating objects have been highlighted in yellow over the range of T_{mb} (main-beam temperature) test-level values for which the virial parameter is less than 2. The *x*–*y* locations of the four 'self-gravitating' leaves labelled with billiard balls are the same as those shown in Fig. 1. The 3D visualizations show position–position–velocity (*p*–*p*–*v*) space. RA, right ascension; dec., declination. For comparison with the ability of dendrograms (**c**) to track hierarchical structure, **d** shows a pseudo-dendrogram of the CLUMPFIND segmentation (**b**), with the same four labels used in Fig. 1 and in **a**. As 'clumps' are not allowed to belong to larger structures, each pseudo-branch in **d** is simply a series of lines connecting the maximum emission value in each clump to the threshold value. A very large number of clumps appears in **b** because of the sensitivity of CLUMPFIND to noise and small-scale structure in the data. In the online PDF version, the 3D cubes (**a** and **b**) can be rotated to any orientation, and surfaces can be turned on and off (interaction requires Adobe Acrobat version 7.0.8 or higher). In the printed version, the front face of each 3D cube (the 'home' view in the interactive online version) corresponds exactly to the patch of sky shown in Fig. 1, and velocity with respect to the Local Standard of Rest increases from front (-0.5 km s^{-1}) to back (8 km s^{-1}).

data, CLUMPFIND typically finds features on a limited range of scales, above but close to the physical resolution of the data, and its results can be overly dependent on input parameters. By tuning CLUMPFIND's two free parameters, the same molecular-line data set[8] can be used to show either that the frequency distribution of clump mass is the same as the initial mass function of stars or that it follows the much shallower mass function associated with large-scale molecular clouds (Supplementary Fig. 1).

Four years before the advent of CLUMPFIND, 'structure trees'[9] were proposed as a way to characterize clouds' hierarchical structure using 2D maps of column density. With this early 2D work as inspiration, we have developed a structure-identification algorithm that abstracts the hierarchical structure of a 3D (*p*–*p*–*v*) data cube into an easily visualized representation called a 'dendrogram'[10]. Although well developed in other data-intensive fields[11,12], it is curious that the application of tree methodologies so far in astrophysics has been rare, and almost exclusively within the area of galaxy evolution, where 'merger trees' are being used with increasing frequency[13].

Figure 3 and its legend explain the construction of dendrograms schematically. The dendrogram quantifies how and where local maxima of emission merge with each other, and its implementation is explained in Supplementary Methods. Critically, the dendrogram is determined almost entirely by the data itself, and it has negligible sensitivity to algorithm parameters. To make graphical presentation possible on paper and 2D screens, we 'flatten' the dendrograms of 3D data (see Fig. 3 and its legend), by sorting their 'branches' to not cross, which eliminates dimensional information on the *x* axis while preserving all information about connectivity and hierarchy. Numbered 'billiard ball' labels in the figures let the reader match features between a 2D map (Fig. 1), an interactive 3D map (Fig. 2a online) and a sorted dendrogram (Fig. 2c).

A dendrogram of a spectral-line data cube allows for the estimation of key physical properties associated with volumes bounded by isosurfaces, such as radius (R), velocity dispersion (σ_v) and luminosity (L). The volumes can have any shape, and in other work[14] we focus on the significance of the especially elongated features seen in L1448 (Fig. 2a). The luminosity is an approximate proxy for mass, such that $M_{lum} = X_{13CO}L_{13CO}$, where $X_{13CO} = 8.0 \times 10^{20}$ cm^2 K^{-1} km^{-1} s (ref. 15; see Supplementary Methods and Supplementary Fig. 2). The derived values for size, mass and velocity dispersion can then be used to estimate the role of self-gravity at each point in the hierarchy, via calculation of an 'observed' virial parameter, $\alpha_{obs} = 5\sigma_v^2 R/GM_{lum}$. In principle, extended portions of the tree (Fig. 2, yellow highlighting) where $\alpha_{obs} < 2$ (where gravitational energy is comparable to or larger than kinetic energy) correspond to regions of *p*–*p*–*v* space where self-gravity is significant. As α_{obs} only represents the ratio of kinetic energy to gravitational energy at one point in time, and does not explicitly capture external over-pressure and/or magnetic fields[16], its measured value should only be used as a guide to the longevity (boundedness) of any particular feature.

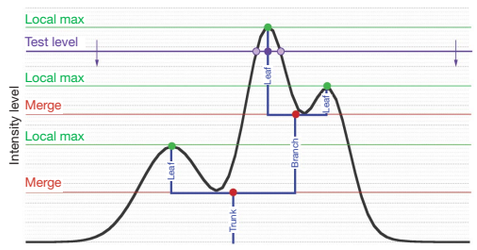

Figure 3 | Schematic illustration of the dendrogram process. Shown is the construction of a dendrogram from a hypothetical one-dimensional emission profile (black). The dendrogram (blue) can be constructed by 'dropping' a test constant emission level (purple) from above in tiny steps (exaggerated in size here, light lines) until all the local maxima and mergers are found, and connected as shown. The intersection of a test level with the emission is a set of points (for example the light purple dots) in one dimension, a planar curve in two dimensions, and an isosurface in three dimensions. The dendrogram of 3D data shown in Fig. 2c is the direct analogue of the tree shown here, only constructed from 'isosurface' rather than 'point' intersections. It has been sorted and flattened for representation on a flat page, as fully representing dendrograms for 3D data cubes would require four dimensions.

©2009 Macmillan Publishers Limited. All rights reserved

Goodman et al. *Nature*, 2009

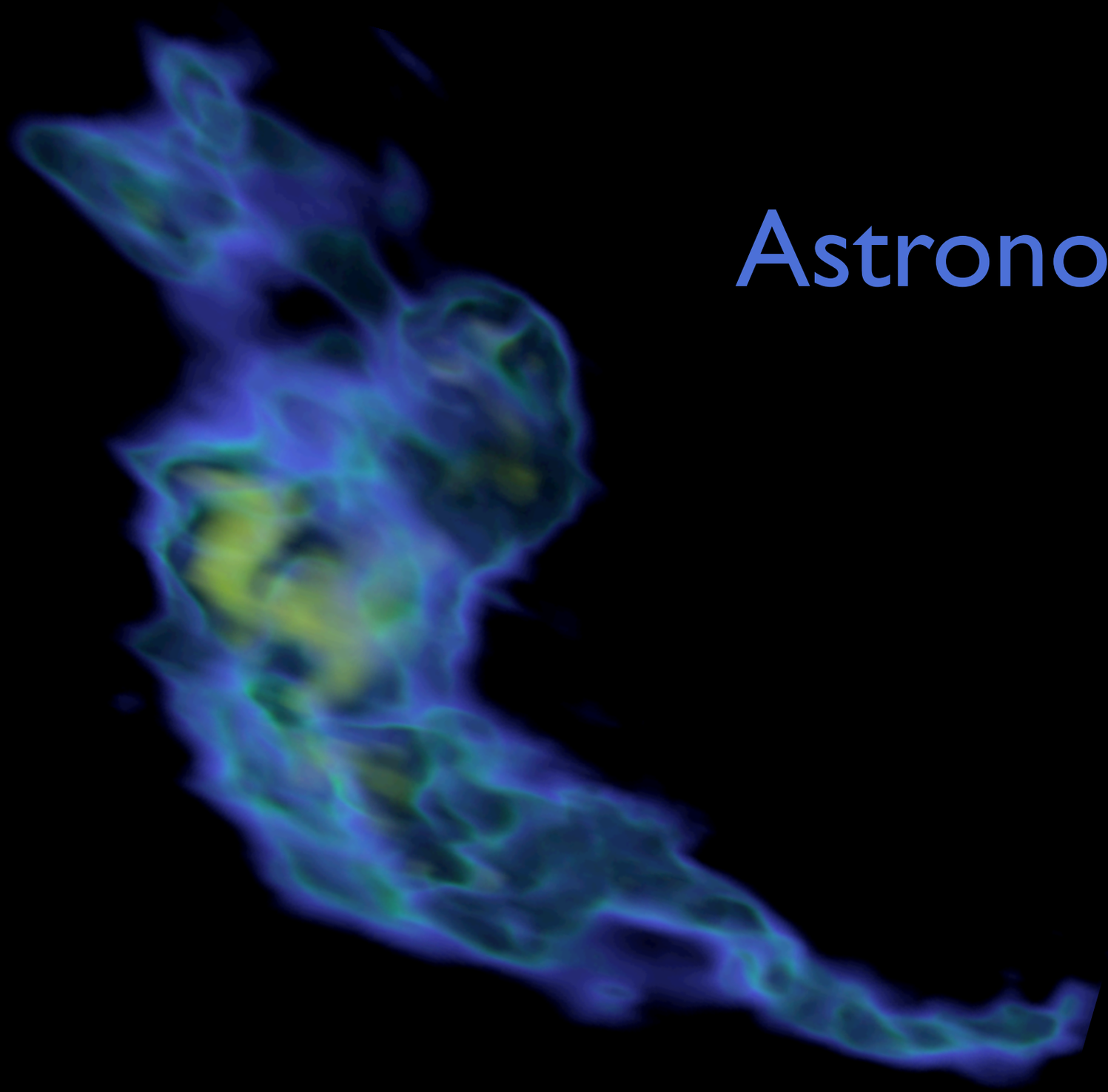

Astronomical Medicine and Beyond

Seamless Astronomy

www.cfa.harvard.edu/~agoodman and worldwidetelescope.org

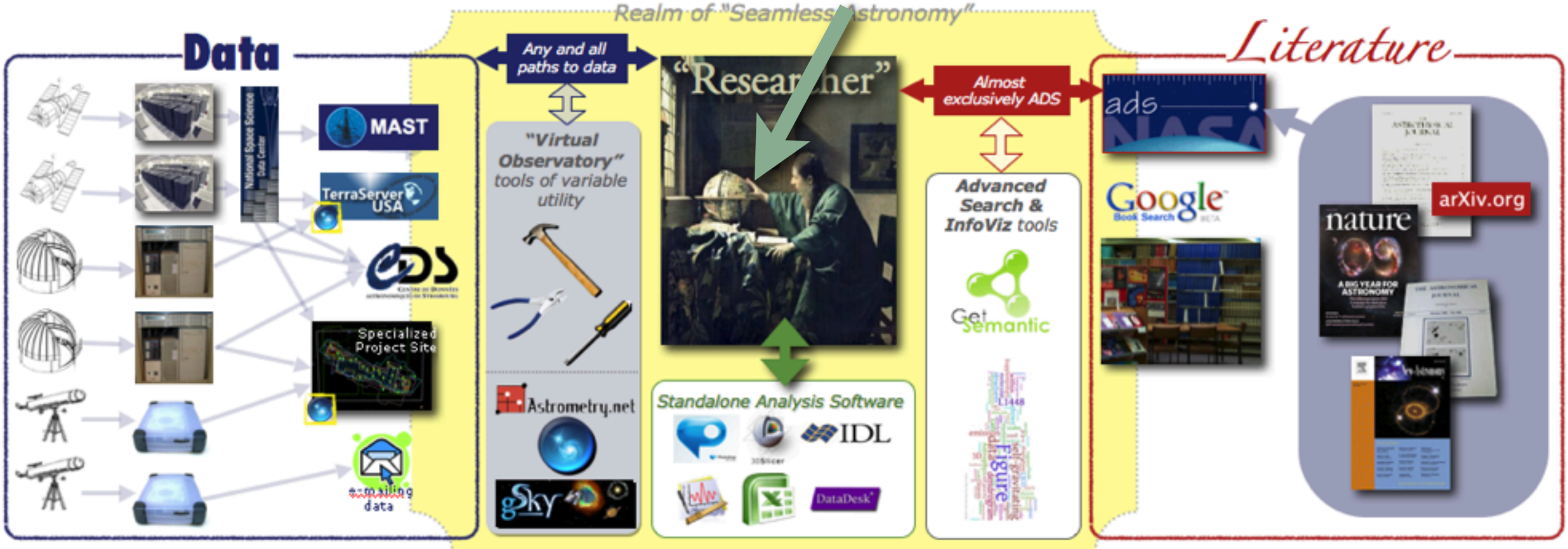

Touching Science

The Scientists' Discovery Room

movie courtesy Daniel Wigdor, equipment now in Chia Shen's SDR lab at SEAS

What about data visualization...

...is easier now than before?

fast computation, animation, 3D

...was easier before than now?

craftsmanship

...should be easier in the future?

modular craftsmanship

"WorldWide Telescope" (from Microsoft Research)

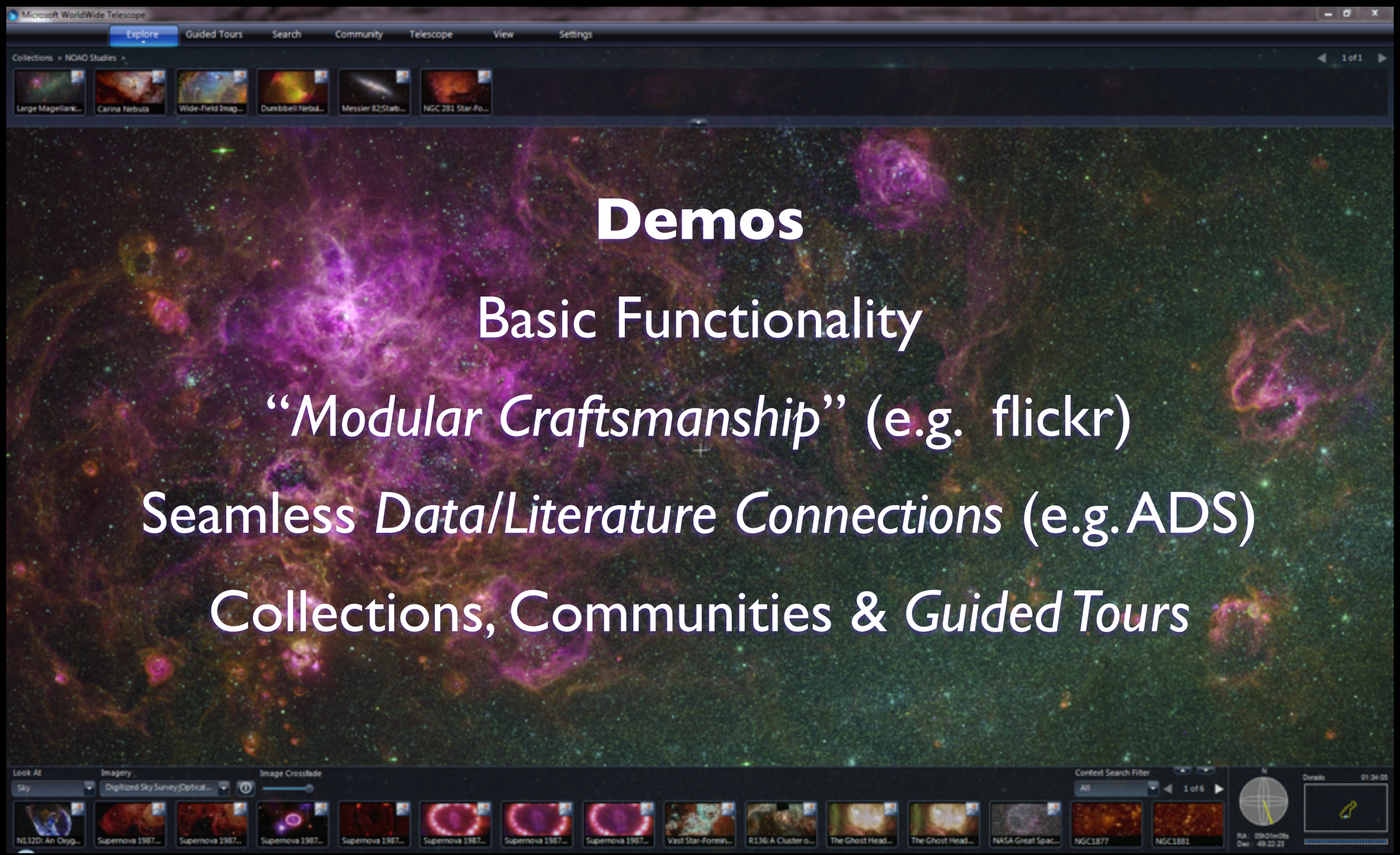

Project Led by Curtis Wong at MSR; software by Jonathan Fay at MSR; AG is "Academic Partner" on the WWT Project

Image ssc2003-06f

http://www.spitzer.caltech.edu/Media/releases/ssc2003-06/ssc200

Google

Spitzer Space Telescope

• Jet Propulsion Laboratory
• California Institute of Technology
• Vision for Space Exploration

NEWSROOM

Press Releases
— Chronological
— By Subject
— Outside Institutions

What's Happening Archive

Visuals
— Image Use Policy

Update Notifications
— Mailing List
— RSS Feed (XML)

References
— Fast Facts
— Press Kit (.pdf)
— Fact Sheet (.pdf)
— Field Guides
— Glossary

Media Contacts

INTRODUCTION | PRESS RELEASE | VISUALS | QUICK FACTS

Credit: NASA/JPL-Caltech/A. Noriega-Crespo (SSC/Caltech), Digital Sky Survey

HH46/47

This image from NASA's Spitzer Space Telescope transforms a dark cloud into a silky translucent veil, revealing the molecular outflow from an otherwise hidden newborn star. Using near-infrared light, Spitzer pierces through the dark cloud to detect the embedded outflow in an object called HH 46/47. Herbig-Haro (HH) objects are bright, nebulous regions of gas and dust that are usually buried within dark clouds. They are formed when supersonic gas ejected from a forming protostar, or embryonic star, interacts with the surrounding interstellar medium. These young stars are often detected only in the infrared.

The Spitzer image was obtained with the infrared array camera. Emission at 3.6 microns is shown as blue, emission from 4.5 and 5.8 microns has been combined as green, and 8.0 micron emission is depicted as red.

HH 46/47 is a striking example of a low-mass protostar ejecting a jet and creating a bipolar, or two-sided, outflow. The central

http://www.flickr.com/photos/66496709@N00/3175344278/

flickr

Signed in as Alyssa_Goodman (1 new) Help Sign Out

Home You Organize Contacts Groups Explore Search

HH4647

Share This

ADD NOTE | SEND TO GROUP | ADD TO SET | BLOG THIS | ALL SIZES | ORDER PRINTS | ROTATE | EDIT PHOTO | DELETE

Uploaded on January 6, 2009
by Alyssa_Goodman

Alyssa_Goodman's photostream

16 uploads

browse

This photo also belongs to:

astrometry (Pool)

Tags

- Astrometrydotnet:version=10145
- Astrometrydotnet:id=alpha-200901-20629873
- Astrometrydotnet:status=solved

Add a tag

Additional Information

- All rights reserved (edit)
- Anyone can see this photo (edit)
- Add to your map
- Taken on December 12, 2003 (edit)
- Photo stats
- Viewed 7 times (Not including you)
- Edit title, description, and tags

Flag your photo

Monday, November 16, 2009

MASSACHUSETTS GENERAL HOSPITAL

April 2009
ISSUE 16

CARDIOVASCULAR IMAGES

A joint publication of the Department of Radiology and Heart Center

New-Onset Chest Pain

Ricardo J. Benenstein, MD, Rahul Kakkar, MD, Wilfred Mamuya, MD, PhD, Suhny Abbara, MD

Clinical History

A 48 year-old woman with a history of mitral valve insufficiency presented to the emergency room with a subacute (4 days) chest pain syndrome. The day of admission, she was awakened from sleep with substernal chest pressure which was non-radiating, worsened with exercise and was relieved by rest. She denied difficulty breathing, palpitations, diaphoresis, or syncope. She was referred to Massachusetts General Hospital, where her presenting EKG showed ST-elevations in V2–V3 and T wave inversions in I and aVL. Her presenting biomarkers were unremarkable. She was given aspirin, metoprolol and intravenous heparin and transferred to the Catheterization Laboratory. Cardiac catheterization revealed an occluded left main (LM) coronary artery, with left anterior descending artery (LAD) and left circumflex artery (LCx) filling from the right coronary artery (RCA). No intervention was performed and medical management with aspirin, beta-blockers, HMG CoA reductase inhibitors and ACE-inhibitors was initiated.

Following catheterization, she continued to have episodes of chest pain with associated ST segment depression and T wave inversion in the anterior leads. A symptom-limited perfusion study was suboptimal, but suspicious for reversible anterior wall myocardial ischemia. A decision was made to proceed with cardiac revascularization with a single bypass graft left internal mammary artery (LIMA) to LAD; and a prospectively triggered dual source 64 slice coronary CTA was requested prior to surgical revascularization to further delineate coronary anatomy and mammary arteries.

Findings

Cardiac CTA revealed a short left main with an absent ostium. The RCA was markedly enlarged, and the LAD and LCx were opacified via collateral flow from a right-sided posterior left ventricular branch (PLVB). All three main coronary arteries were free of evidence of epicardial coronary artery disease. This constellation of findings is consistent with congenital left main coronary atresia (LMCA).

Discussion

LMCA is a rare coronary anomaly in which there is no left main ostium, and the proximal left main trunk ends blindly. Blood flows retrograde from the right coronary artery to the left circulation via collaterals. The collateral vessels feeding the left coronary system may include the conal, intraseptal, apical, anterior, and posterior ventricular arteries. Most patients are symptomatic at the time of diagnosis; with syncope, failure to thrive and myocardial infarction being the commonest presentation in the pediatric population. Older patients usually present with complaints of exertional dyspnea or angina in the absence of atherosclerotic disease, and sudden death is a rare presenting symptom. Medical therapy does not appear to be helpful.

INSIDE THE MGH

> MGH Radiology

> MGH Heart Center

QUICK LINKS

> Download pdf version of this article

> Refer a patient for an imaging exam

> Refer a patient to the Heart Center

> Archived Issues of Cardiovascular Images

> Bookmark this site

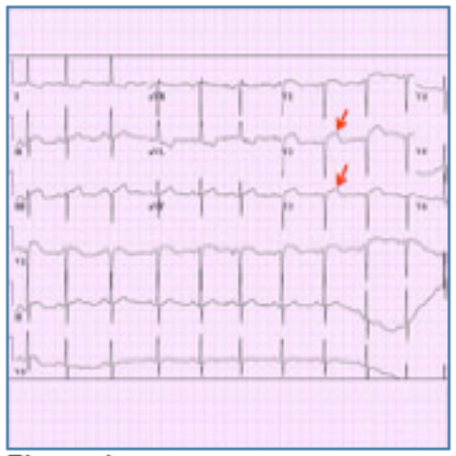

Figure 1.

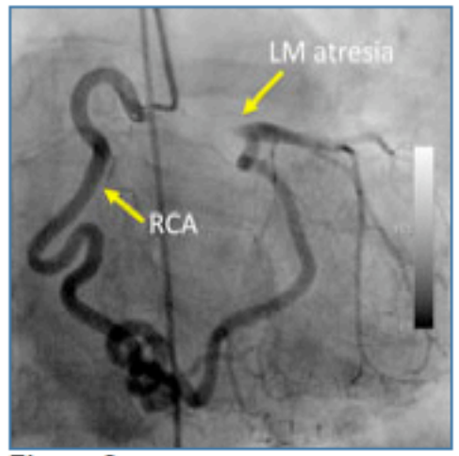

Figure 2.

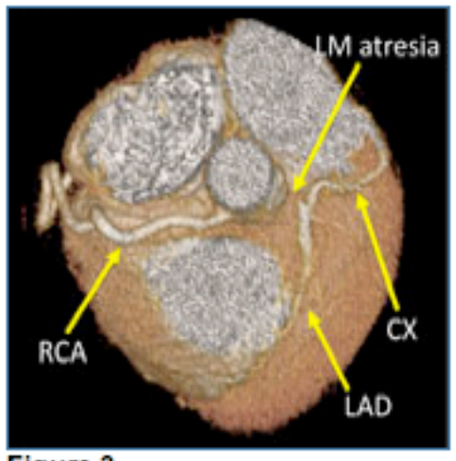

Figure 3.

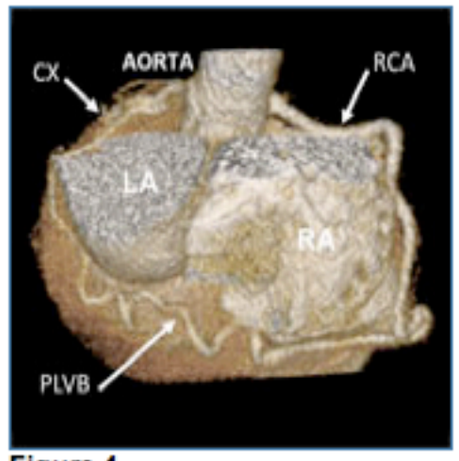

Figure 4.

(Click on images to enlarge)

Figure 1. Presenting EKG with ST-T elevation in V2 – V3 (arrows).

Figure 2. CATH: RAO view showing an enlarged RCA with a large terminal PLV branch. The left main appears to be occluded LM. The LCx and LAD fill with retrograde flow from the PLV branch.

Figure 3. 3D volume rendered CTA showing the LM Atresia.

Figure 4. 3D volume rendered CTA showing an enlarged RCA with a large terminal PLV branch connecting to the LCx.

How would this be as an interactive tour?

http://www.mgh-cardiovascimages.org/index.php?src=gendocs&ref=cv_april_2009

Seamless Astronomy

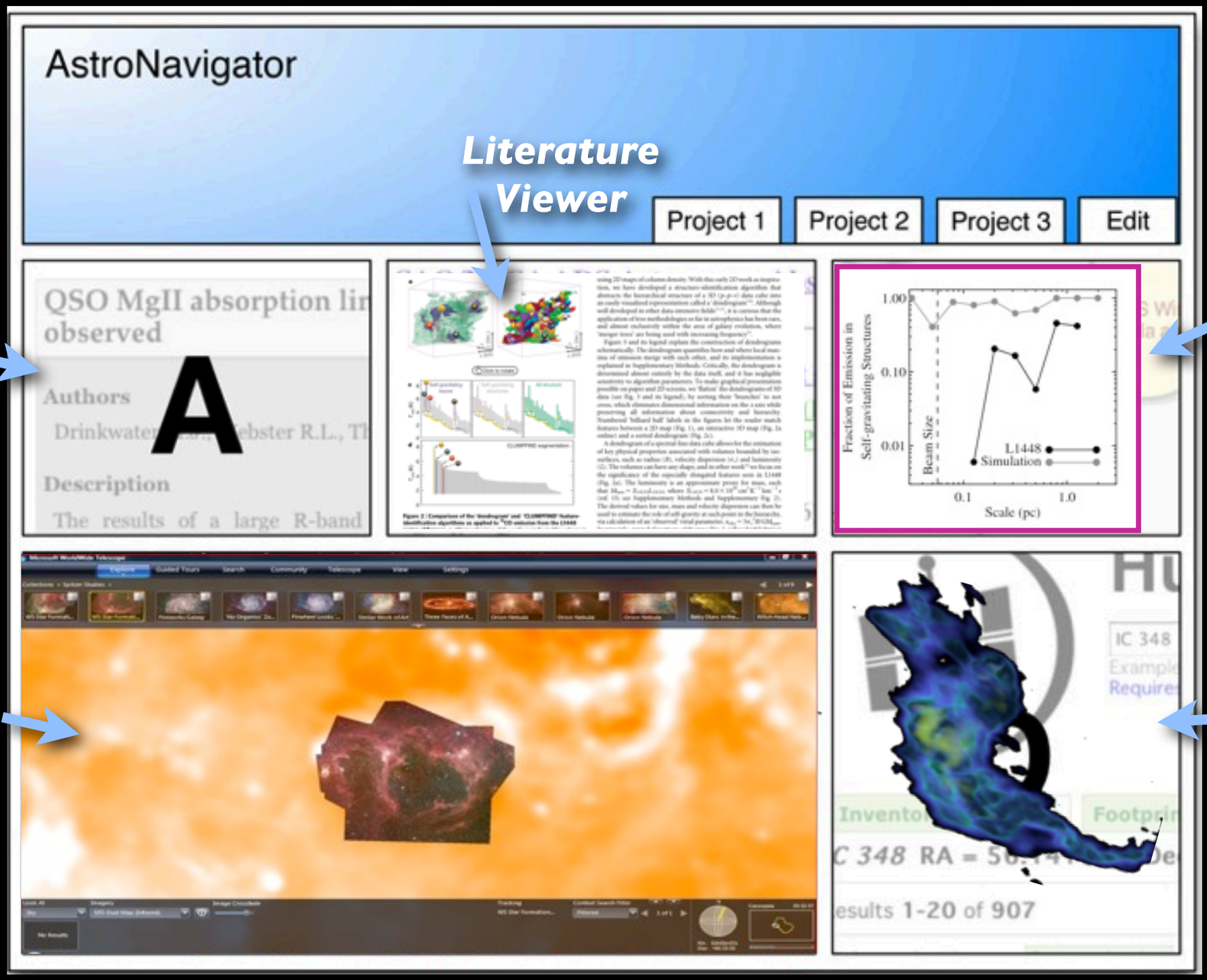

Semantic Search

Info-Viz for Analytics

Data Viewer (e.g. WWT)

ArcGIS Viewer

Mockup based on work of Eli Bressert, excerpted from NASA AISRP proposal by Goodman, Muench, Christian, Conti, Kurtz, Burke, Accomazzi, McGuinness, Hendler & Wong, 2008

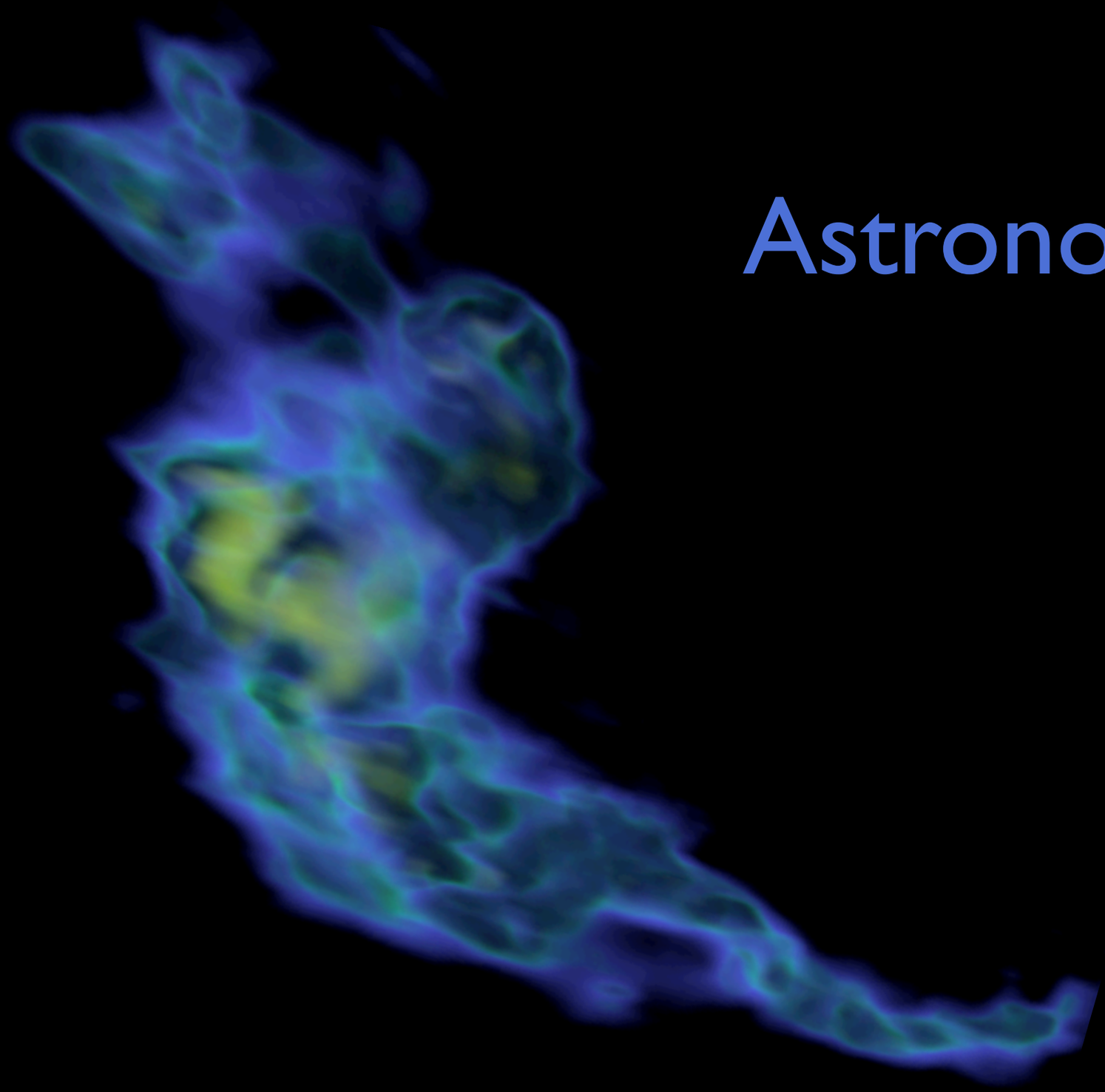

Astronomical Medicine and Beyond

Alyssa A. Goodman

Professor of Astronomy
& Founding Director of the
Initiative in Innovative Computing,
Harvard University

Scholar-in-Residence,
WGBH Boston

worldwidetelescope.org